Naval Research Laboratory

Washington, DC 20375-5320

NRL/MR/6110--12-9397

2011 ESTCP Live Site Demonstrations Vallejo, CA

ESTCP MR-1165
Demonstration Data Report
Former Mare Island Naval Shipyard
MTADS Discrimination Array (TEMTADS) Survey

James B. Kingdon
Thomas H. Bell

SAIC, Inc. - ASAD
Arlington, Virginia

Mark J. Howard
Cora E. Blits

NAEVA Geophysics, Inc.
Charlottesville, Virginia

Glenn R. Harbaugh
Daniel A. Steinhurst

Nova Research, Inc.
Alexandria, Virginia

April 5, 2012

REPORT DOCUMENTATION PAGE

Form Approved
OMB No. 0704-0188

1. REPORT DATE *(DD-MM-YYYY)*	**2. REPORT TYPE**	**3. DATES COVERED** *(From - To)*
05-04-2012	Memorandum Report	June 2011 - August 2011

4. TITLE AND SUBTITLE
2011 ESTCP Live Site Demonstrations
Vallejo, CA
ESTCP MR-1165
Demonstration Data Report
Former Mare Island Naval Shipyard
MTADS Discrimination Array (TEMTADS) Survey

5a. CONTRACT NUMBER
N00173-05-C-2063

5b. GRANT NUMBER

5c. PROGRAM ELEMENT NUMBER
0603851D8Z

6. AUTHOR(S)

James B. Kingdon,* Thomas H. Bell,* Mark J. Howard,†
Cora E. Blits,† Glenn R. Harbaugh,‡ and Daniel A. Steinhurst‡

5d. PROJECT NUMBER
MR-1165

5e. TASK NUMBER

5f. WORK UNIT NUMBER
61-5802-A-1-5

7. PERFORMING ORGANIZATION NAME(S) AND ADDRESS(ES)

Naval Research Laboratory, Code 6110
4555 Overlook Avenue, SW
Washington, DC 20375-5320

8. PERFORMING ORGANIZATION REPORT NUMBER

NRL/MR/6110--12-9397

9. SPONSORING / MONITORING AGENCY NAME(S) AND ADDRESS(ES)

Environmental Security Technology Certification Program (ESTCP) Program Office
901 North Stuart Street, Suite 303
Arlington, VA 22203

10. SPONSOR / MONITOR'S ACRONYM(S)
ESTCP

11. SPONSOR / MONITOR'S REPORT NUMBER(S)

12. DISTRIBUTION / AVAILABILITY STATEMENT

Approved for public release; distribution is unlimited.

13. SUPPLEMENTARY NOTES

*SAIC, Inc. - ASAD, 4001 N. Fairfax Drive, 4th Floor, Arlington, VA 22203
†NAEVA Geophysics, Inc., P.O. Box 7325, Charlottesville, VA 22906
‡Nova Research, Inc., 1900 Elkin Street, Suite 230, Alexandria, VA 22308

14. ABSTRACT

The MTADS Discrimination Array (TEMTADS) 5×5 array was demonstrated at the former Mare Island Naval Shipyard, CA, during July 2011 as part of the ESTCP Live Site Demonstrations. The TEMTADS 5×5 array is vehicle-towed with array position and orientation determined with cm-level GPS. TEM data are collected at each target location while the vehicle and sensor array are stopped, with an on-target collection time of approximately 1.5 minutes. The data are inverted to determine the principal axis eddy current decay functions of the targets. Classification is based on comparing the eddy current decay functions for each target with those of the various munitions targets of interest at the site, as well as a variety of clutter items that are representative of the non-hazardous metal debris at the site. We report the classification performance results with the TEM array for approximately 2,100 unknown targets at the former Mare Island Naval Shipyard, CA.

15. SUBJECT TERMS

Discrimination	Multi-sensor Towed Array Detection System (MTADS)	TEMTADS
Classification	Electromagnetic induction (EMI)	Former Mare Island Naval Shipyard, CA
Unexploded ordnance (UXO)	Transient electromagnetic induction (TEM)	

16. SECURITY CLASSIFICATION OF:			**17. LIMITATION OF ABSTRACT**	**18. NUMBER OF PAGES**	**19a. NAME OF RESPONSIBLE PERSON**
					B.J. Spargo, NRL, Code 6110
a. REPORT	**b. ABSTRACT**	**c. THIS PAGE**	Unclassified Unlimited	61	**19b. TELEPHONE NUMBER** *(include area code)*
Unclassified Unlimited	Unclassified Unlimited	Unclassified Unlimited			(202) 404-6392

Standard Form 298 (Rev. 8-98)
Prescribed by ANSI Std. Z39.18

Contents

Figures viii

Tables x

Acronyms xi

1.0 Introduction 1

1.1 Organization of this document 1

1.2 Demonstration Background and Objectives 1

1.3 Specific Objectives of Demonstration 1

2.0 Technology 1

2.1 Technology Description 1

2.1.1 EMI Sensors 1

2.1.2 Sensor Array 5

2.1.3 Application of the Technology 9

2.1.4 Development of the Technology 10

2.2 Advantages and Limitations of the Technology 11

3.0 Performance Objectives 11

3.1 Objective: Site Coverage 11

3.1.1 Metric 11

3.1.2 Data Requirements 11

3.1.3 Success Criteria 12

3.2 Objective: Instrument verification Strip Results 13

3.2.1 Metric 13

3.2.2 Data Requirements 13

3.2.3 Success Criteria 13

3.3 Objective: Location Accuracy 13
3.3.1 Metric 13
3.3.2 Data Requirements 13
3.3.3 Success Criteria 13
3.4 Objective: Depth Accuracy 14
3.4.1 Metric 14
3.4.2 Data Requirements 14
3.4.3 Success Criteria 14
3.5 Objective: Production Rate 14
3.5.1 Metric 14
3.5.2 Data Requirements 14
3.5.3 Success Criteria 14
3.6 Objective: Data Throughput 14
3.6.1 Metric 15
3.6.2 Data Requirements 15
3.6.3 Success Criteria 15
3.7 Objective: Reliability and Robustness 15
3.7.1 Data Requirements 15
4.0 Site Description 15
5.0 Test Design 15
5.1 Conceptual Experimental Design 15
5.2 Site Preparation 16
5.3 Systems Specification 16
5.3.1 MTADS Tow Vehicle 16

5.3.2 RTK GPS System 16
5.3.3 Time-Domain Electromagnetic Sensor 17
5.4 Calibration Activities 18
5.4.1 TEMTADS Sensor Calibration 18
5.4.2 Background Data 18
5.4.3 Instrument Verification Strip Data 20
5.4.4 Geophysical Prove-Out 23
5.5 Data Collection Procedures 25
5.5.1 Scale of Demonstration 25
5.5.2 Sample Density 25
5.5.3 Quality Checks 25
5.5.4 Data Handling 28
5.6 Anomaly Positioning in the PMA 28
5.7 Validation 29
6.0 Data Analysis Plan 30
6.1 Preprocessing 30
6.2 Parameter Estimation 30
6.3 Data Product Specifications 32
7.0 Performance Assessment 32
7.1 Objective: Site Coverage 32
7.1.1 Metric 32
7.1.2 Data Requirements 32
7.1.3 Success Criteria 33
7.1.4 Results 33

7.2 Objective: Instrument Verification Strip Results 34
7.2.1 Metric 34
7.2.2 Data Requirements 34
7.2.3 Success Criteria 34
7.2.4 Results 34
7.3 Objective: Location Accuracy 34
7.3.1 Metric 34
7.3.2 Data Requirements 35
7.3.3 Success Criteria 35
7.3.4 Results 35
7.4 Objective: Depth Accuracy 35
7.4.1 Metric 35
7.4.2 Data Requirements 35
7.4.3 Success Criteria 35
7.4.4 Results 35
7.5 Objective: Production Rate 35
7.5.1 Metric 36
7.5.2 Data Requirements 36
7.5.3 Success Criteria 36
7.5.4 Results 36
7.6 Objective: Data Throughput 36
7.6.1 Metric 36
7.6.2 Data Requirements 36
7.6.3 Success Criteria 36

7.6.4 Success Criteria 37
7.7 Objective: Reliability and Robustness 37
7.7.1 Data Requirements 37
7.7.2 Results 37
8.0 Cost Assessment 38
9.0 Schedule of Activities 40
10.0 Management and Staffing 40
11.0 References 41
Appendix A. Health and Safety Plan (HASP) A-1
A.1 Directions to the Hospital A-1
A.2 Emergency Telephone Numbers A-2
Appendix B. Points of Contact B-1
Appendix C. Data Formats C-1
C.1 Position / orientation data file (*.GPS) C-1
C.2 TEM Data file (*.TEM) C-1
C.3 Leveled Data file C-3

Figures

Figure 2-1 – Construction details of an individual EMI sensor (left panel) and the assembled sensor with end caps attached (right panel). 2

Figure 2-2 – Measured transmit current (on-time upper panel, off-time second panel), full measured signal decay (third panel), and gated decay (fourth panel) as discussed in the text. 3

Figure 2-3 – Measured response from a 2-in steel sphere placed 25 cm from the sensor. Decays 1, 1001, 2001, and 3001 from a series that started from a cold start are plotted along with the expected response from this target. 4

Figure 2-4 – Measured response from three calibration coils and the background response between measurements plotted on a semi-log plot to emphasize the exponential nature of the decay. The decay time constants extracted from the measurements are listed in the legend. 4

Figure 2-5 – Sketch of the EMI sensor array showing the position of the 25 sensors and the three GPS antennae. 5

Figure 2-6 – Sensor array mounted on the MTADS EMI sensor platform. 6

Figure 2-7 – Comparison of the response of the array members. The measured decay from a 2-in steel sphere held 30 cm below each sensor in turn is plotted. The decays are indistinguishable. 6

Figure 2-8 – The response of nine of the individual sensors to a 40-mm projectile located under the center of the array. 7

Figure 2-9 – Derived response coefficients for a 40-mm projectile using the measurements of which the decays shown in Figure 2-8 are a subset. 8

Figure 2-10– Derived response coefficients from a cued measurement over "Cylinder E" in the test field. 8

Figure 2-11 – Three sets of βs derived from three measurements over a 4.2-in mortar baseplate at different position/orientation pairs. 9

Figure 5-1 – Field Testing Activities Schedule for Mare Island, CA 16

Figure 5-2 – MTADS tow vehicle and magnetometer array. 17

Figure 5-3 – Intra- and inter- daily variations in the response of the TEMTADS to background anomaly-free areas through the duration of the demonstration at fMINSY. The points represent the average measured signal of the 25 monostatic quantities, while the bars represent the standard deviation of those quantities (i.e. 1σ about the mean). 19

Figure 5-4 – Derived response coefficients for item 1, the superISO, emplaced in the IVS..... 21

Figure 5-5 – Amplitude variations at 0.042 ms in the derived response coefficients for all items emplaced in the IVS (right panel). β_1 is in red; β_2 is in green; and β_3 is in blue. 21

Figure 5-6 – Position errors for the SuperISO emplaced in the IVS (left panel). Easting data are in black and Northing data are in red. Depth errors for the same item (right panel)..... 22

Figure 5-7 – Position error statistics for the three items emplaced in the IVS (left panel). Easting data are in black and Northing data are in red. Depth error statistics for the same items (right panel). 22

Figure 5-8 – TEMTADS Operator Monostatic Contour Plot Display with a Single Anomaly Well-Centered under the Array. 26

Figure 5-9 – Monostatic contour plot of a well-centered anomaly. 27

Figure 5-10 – Monostatic decay plots for a) a well-centered anomaly and b) a background (no-anomaly) area with a malfunctioning receiver element (#20)..... 27

Figure 5-11 – fMINSY TEMTADS Initial Fit Results, Position Error (Horizontal Offset) from the Provided Location. 29

Figure 6-1 – Principal axis polarizabilities for a 0.5 cm thick by 25 cm long by 15 cm wide mortar fragment. 32

Figure 9-1 – Schedule of all demonstration activities including deliverables. 40

Figure 10-1 – Management and Staffing Wiring Diagram. 40

Figure A-1 – Area map showing the location of the Sutter Medical Center with respect to the work site. A-2

Tables

Table 3-1 – Performance Objectives for this Demonstration 12

Table 5-1 – Summary of the Daily Variation in the Mean and Standard Deviation of the Signals Measured for the Background Areas 19

Table 5-2 – Details of Former Mare Island Naval Shipyard IVS 20

Table 5-3 – Summary of the Amplitude Variations at 0.042 ms in the Derived Response Coefficients for All Items Emplaced in the IVS. 21

Table 5-4 – Summary of Position and Depth Error Statistics for all items emplaced in the IVS. 23

Table 5-5 – fMINSY GPO Details 24

Table 5-6 – Reacquisition Offset for Control Point SE MARE 24

Table 7-1 – Performance Results for this Demonstration. 33

Table 8-1 – Tracked Costs 39

Table A-1 – Emergency Contact Numbers A-3

Acronyms

Abbreviation	Definition
AMTADS	Airborne Multi-sensor Towed Array Detection System
APG	Aberdeen Proving Ground
ASCII	American Standard Code for Information Interchange
ATC	Aberdeen Test Center
CD-R	Compact Disk - Recordable
DAQ	Data Acquisition (System)
DAS	Data Analysis System
DVD-R	Writable digital versatile disc
EMI	Electro-Magnetic Induction
ESTCP	Environmental Security Technology Certification Program
FQ	Fix Quality
FUDS	Formerly -Used Defense Site
GPS	Global Positioning System
HASP	Health and Safety Plan
Hz	Hertz
IVS	Instrument Verification Strip
(f)MINSY	(former) Mare Island Naval Shipyard, located in Vallejo, CA
MR	Munitions Response
MTADS	Multi-sensor Towed Array Detection System
NMEA	National Marine Electronics Association
NRL	Naval Research Laboratory
Pd	Probability of Detection
PMA	Production and Manufacuturing Area of fMINSY
POC	Point of Contact
(PTNL,)AVR	Time, Yaw, Tilt, Range for Moving Baseline RTK NMEA-0183 message
(PTNL,)GGK	Time, Position, Position Type, DOP NMEA-0183 message
QC	Quality Control
ROC	Receiver Operating Characteristic
RTK	Real Time Kinematic
Rx	Receiver
SAIC	Science Applications International Corporation
SERDP	Strategic Environmental Research and Development Program
SLO	San Luis Obispo
TEM	Time-domain Electro-Magnetic
TEMTADS	Time-domain Electro-Magnetic MTADS
Tx	Transmit(ter)
UXO	Unexploded Ordnance

1.0 INTRODUCTION

1.1 ORGANIZATION OF THIS DOCUMENT

The results for the demonstration of the Multi-sensor Towed Array Detection System (MTADS) EMI Array for Cued Discrimination, or TEMTADS, participation in the Environmental Security Technology Certification Program (ESTCP) Live Site Demonstrations at the former Mare Island Naval Shipyard (MINSY), located in Vallejo, CA in 2011 are presented in this document. To limit the repetition of information, demonstration- and site- specific information that is presented elsewhere such as in the ESTCP Live Site Demonstrations Plan [1] is noted and not repeated in this document.

1.2 DEMONSTRATION BACKGROUND AND OBJECTIVES

Please refer to the ESTCP Live Site Demonstrations Plan [1].

1.3 SPECIFIC OBJECTIVES OF DEMONSTRATION

As part of NRL's ESTCP-funded Live Site Demonstrations, the Naval Research Laboratory (NRL) conducted a cued discrimination survey within the 61 acre Production and Manufacturing Area (PMA) at the former MINSY (fMINSY) demonstration site of 2,061 previously-identified anomalies. The survey was conducted using the NRL TEMTADS array. Characterization of the system response to the site-specific Targets of Interest (TOIs) was limited to the contents of a pre-existing Geophysical Prove-Out (GPO) and our existing library. All data collected in the course of the demonstration were collected in accordance with the overall demonstration objectives and demonstration plan. This report documents the results of the TEMTADS demonstration at fMINSY.

2.0 TECHNOLOGY

2.1 TECHNOLOGY DESCRIPTION

2.1.1 EMI Sensors

The EMI sensor used in the TEMTADS array is based on the Navy-funded Advanced Ordnance Locator (AOL), developed by G&G Sciences. The AOL consists of three transmit coils arranged in a 1-m cube; we have adopted the transmit (Tx) and receive (Rx) subsystems of this sensor directly, converted to a 5 x 5 array of 35 cm square sensors, and made minor modifications to the control and data acquisition computer to make it compatible with our deployment scheme.

A photograph of an individual sensor element under construction is shown in the left panel of Figure 2-1. The transmit coil is wound around the outer portion of the form and is 35 cm on a side. The 25-cm receive coil is wound around the inner part of the form which is re-inserted into the outer portion. An assembled sensor with the top and bottom caps used to locate the sensor in the array is shown in the right panel of Figure 2-1.

Manuscript approved January 23, 2012.

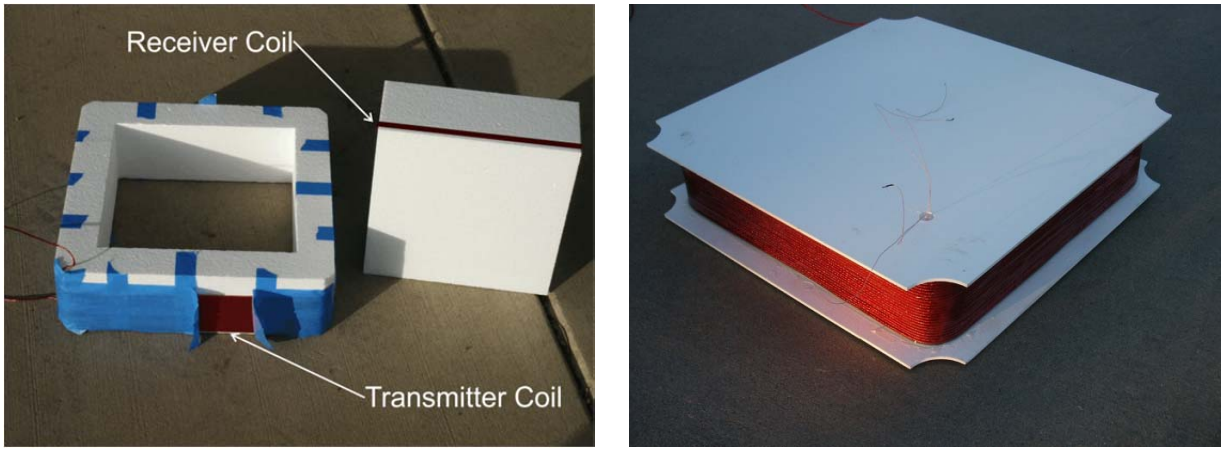

Figure 2-1 – Construction details of an individual EMI sensor (left panel) and the assembled sensor with end caps attached (right panel).

Decay data are collected with a 500 kHz sample rate until 25 ms after turn off of the excitation pulse. This results in a raw decay of 12,500 points; too many to be used practically. These raw decay measurements are grouped into 122 logarithmically-spaced "gates" with center times ranging from 25 μs to 24.375 ms with 5% widths and are saved to disk. Examples of the measured transmit pulse, raw decay, and gated decay are shown in Figure 2-2.

The individual sensors (consisting of transmit electronics, transmit and receive coils, pre-amp, and digitizer) were characterized at G&G Sciences before approval was given for construction of the array. Examples of the characterization data are shown in Figure 2-3 and Figure 2-4. System stability is demonstrated in Figure 2-3 which plots the normalized (by measured transmit current) response of a 2-in steel ball at a 25 cm separation from the sensor. The data plotted are decays 1, 1001, 2001, and 3001 in a continuously-triggered series that began from a cold start and ran for 2.5 hours. For comparison purposes, the expected response from this sphere is plotted in black. As can be seen, the sensor exhibits excellent stability which will be important for the cued deployment planned.

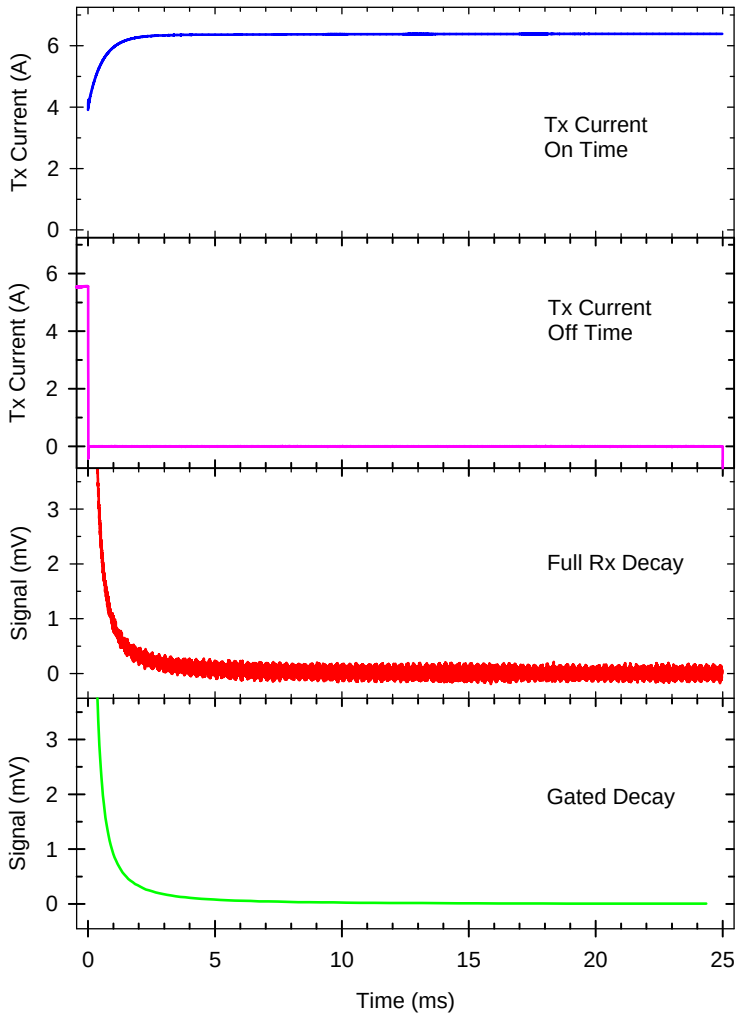

Figure 2-2 – Measured transmit current (on-time upper panel, off-time second panel), full measured signal decay (third panel), and gated decay (fourth panel) as discussed in the text.

The second important characterization test was sensor response linearity. Since we collect decay data to late times and over several orders of magnitude in amplitude, the linearity of system response is very important. To characterize this property of the sensor, we constructed a series of copper coils with nominal decay time constants of 2, 4, and 6 ms. The responses of the three coils are shown in Figure 2-4 which plots the measured decays on semi-log axes. After a transient at early times, the decays exhibit clean exponential behavior with measured decay times of 1.8, 3.3, and 5.8 ms. Careful calculation of the expected decay times at the temperature at which the tests were conducted results in expected values of 1.82, 3.26, and 5.73 ms; the measured values are in excellent agreement with these.

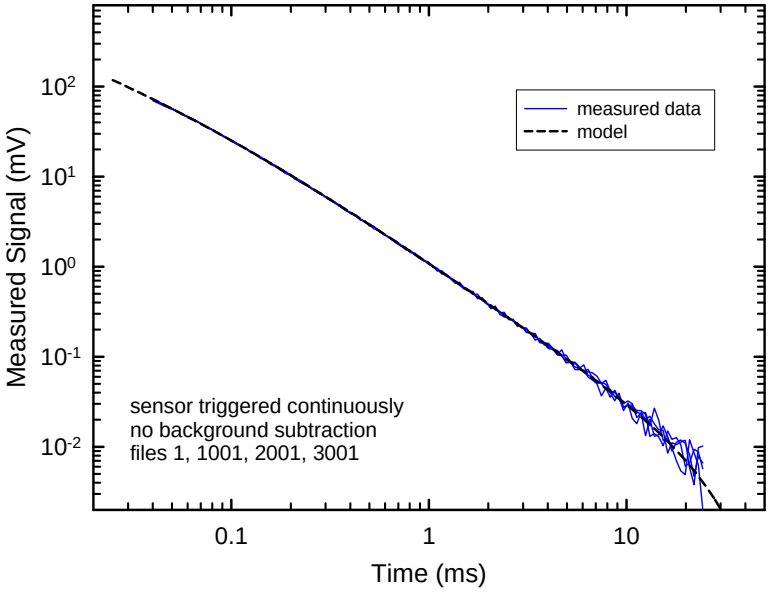

Figure 2-3 – Measured response from a 2-in steel sphere placed 25 cm from the sensor. Decays 1, 1001, 2001, and 3001 from a series that started from a cold start are plotted along with the expected response from this target.

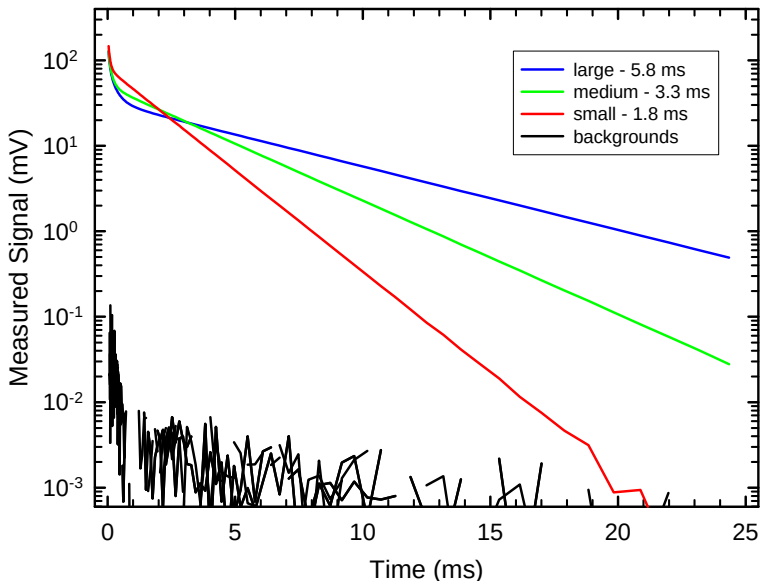

Figure 2-4 – Measured response from three calibration coils and the background response between measurements plotted on a semi-log plot to emphasize the exponential nature of the decay. The decay time constants extracted from the measurements are listed in the legend.

2.1.2 Sensor Array

The twenty-five individual sensors are arranged in a 5 x 5 array as shown in Figure 2-5. The center-to-center distance is 40 cm yielding a 2 m x 2 m array. Also shown in Figure 2-5 is the position of the three GPS antennae that are used to determine the location and orientation of the array for each cued measurement. A picture of the array mounted on the MTADS EMI sensor platform is shown in Figure 2-6.

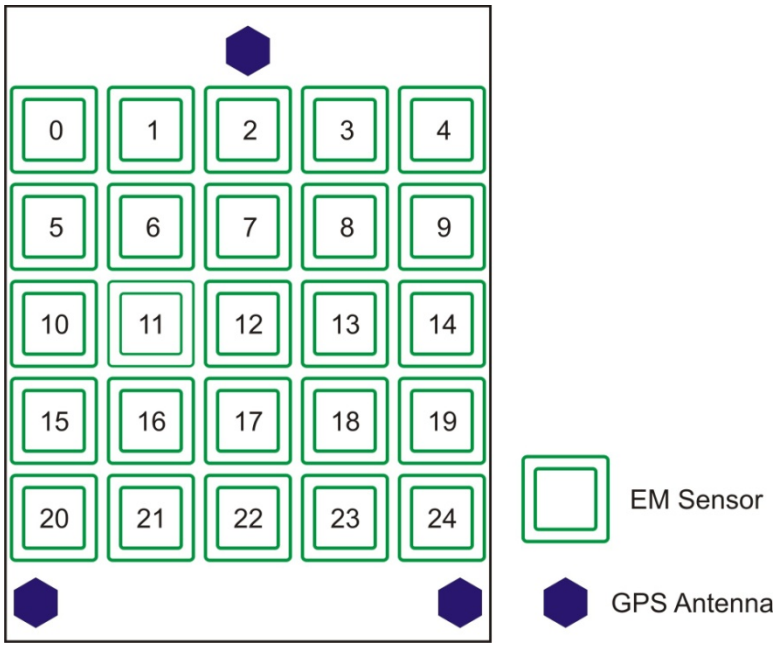

Figure 2-5 – Sketch of the EMI sensor array showing the position of the 25 sensors and the three GPS antennae.

After assembly of the array, a number of array calibration measurements were performed. The first task was to ensure that each of the individual sensors had an equivalent response. A jig was constructed that allowed us to mount a 2-in steel sphere 30 cm below each array element in turn. Data collected using this jig are shown in Figure 2-7. As can be seen, the measured decays from each of the sensors plotted are indistinguishable.

After this, the assembled array was used to measure the response of a number of inert ordnance items and simulants both mounted on a test stand and mounted on the sensor platform in our test field. For each series of measurements with the full array, we cycle through the sensors transmitting from each in turn. After each excitation pulse, we record the response of all twenty-five receive coils. Thus, there are 625 (25 x 25) individual transmit/receive pairs recorded, making it difficult to present a full measurement in any coherent way. In Figure 2-8, we plot nine of the transmit/receive pairs resulting from excitation of a 40-mm projectile located under

the center of the array. The decays plotted correspond to the signal received on the nine central sensors (reference Figure 2-5 for the sensor numbering) when that sensor transmits. In other words, the results of nine individual monostatic measurements are presented.

Figure 2-6 – Sensor array mounted on the MTADS EMI sensor platform.

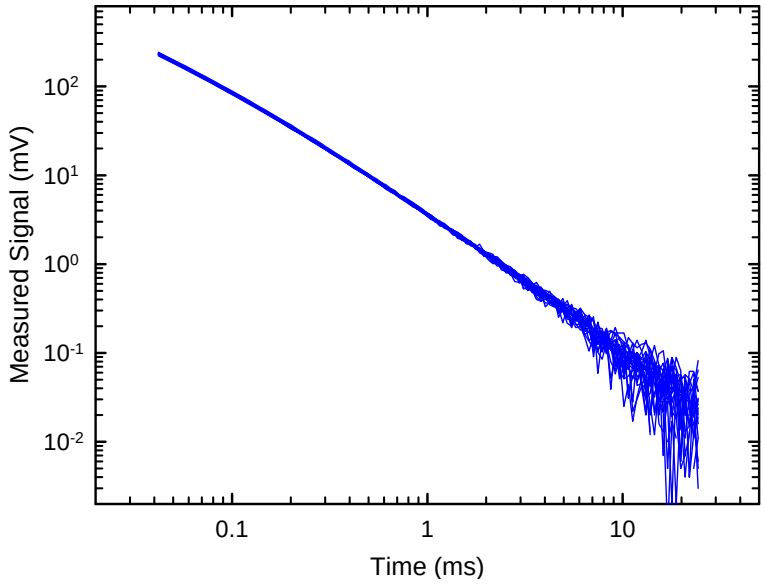

Figure 2-7 – Comparison of the response of the array members. The measured decay from a 2-in steel sphere held 30 cm below each sensor in turn is plotted. The decays are indistinguishable.

All 625 measurements are used for the inversion to recover target parameters. The inversion results for the decay data shown in Figure 2-8 are shown in Figure 2-9. As we expect for an object with axial symmetry such as a 40-mm projectile, we recover one large response coefficient and two equal, but smaller ones. These response coefficients will be the basis of the discrimination decisions in this demonstration. Derived βs for "Cylinder E" (3-in x 12-in steel cylinder) in the test field are shown for comparison in Figure 2-10.

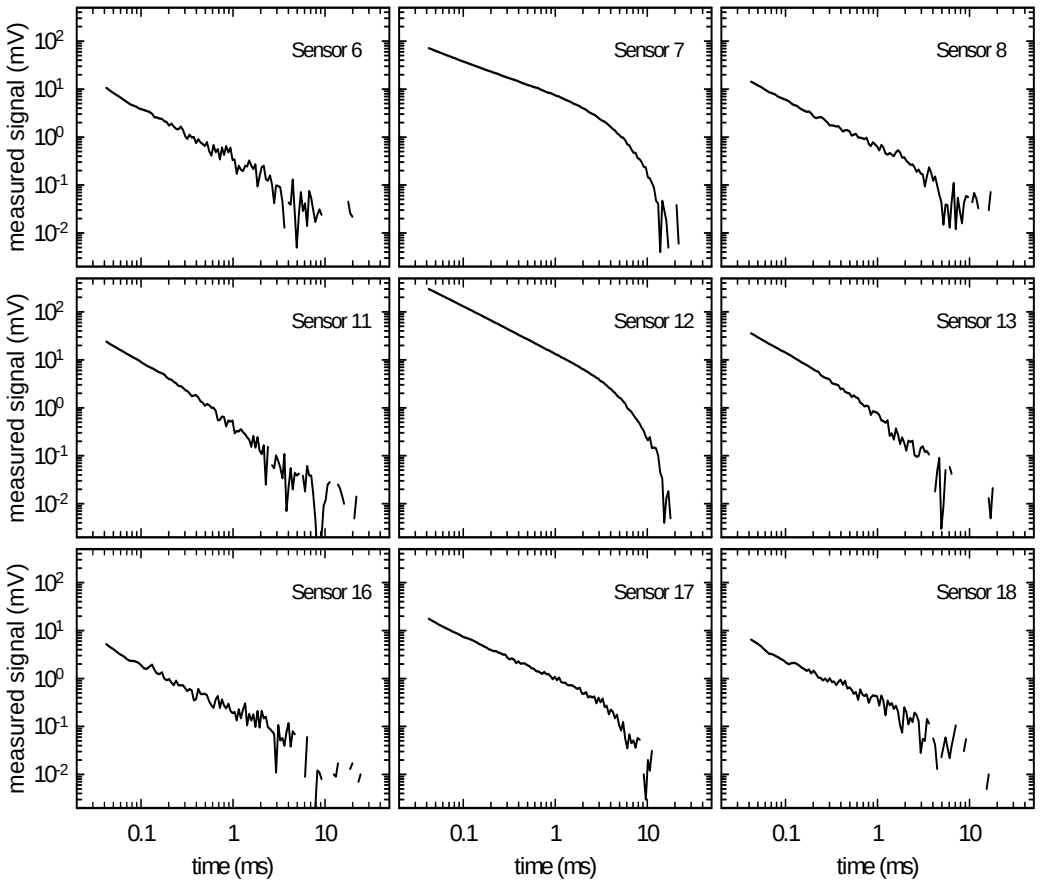

Figure 2-8 – The response of nine of the individual sensors to a 40-mm projectile located under the center of the array.

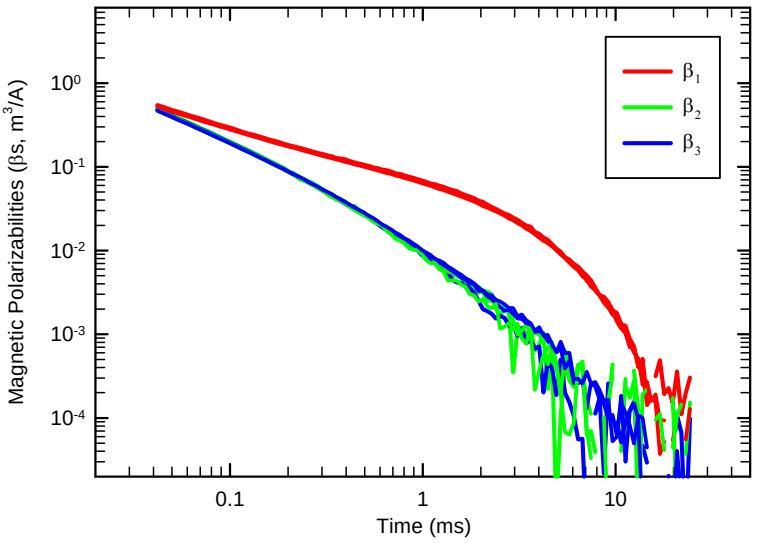

Figure 2-9 – Derived response coefficients for a 40-mm projectile using the measurements of which the decays shown in Figure 2-8 are a subset.

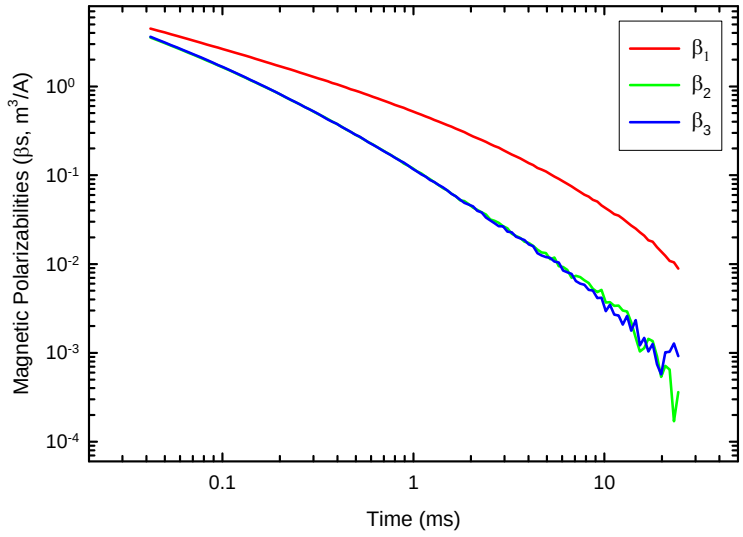

Figure 2-10– Derived response coefficients from a cued measurement over "Cylinder E" in the test field.

The final array characterization test was to confirm that the response coefficients we recover are invariant to object position and orientation under the array. Figure 2-11 shows the derived βs plotted for a 4.2-in mortar baseplate after measurements at three position/orientation pairs. As can be seen, the inversion results are robust to variation in the object's position and orientation.

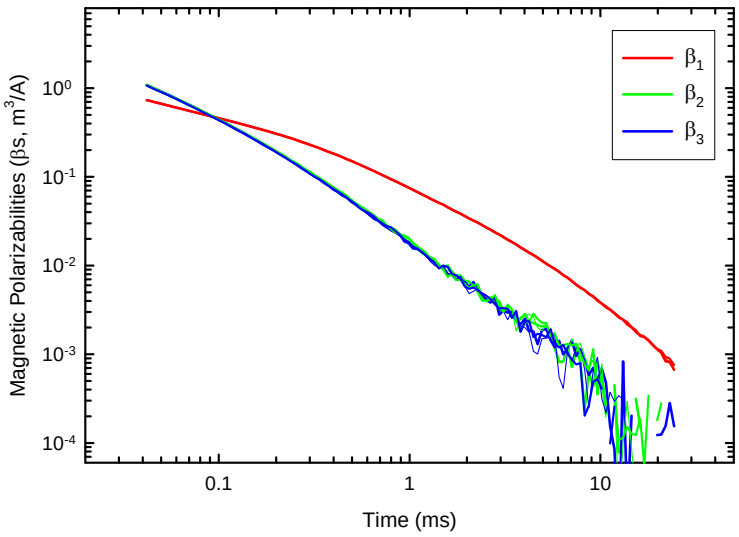

Figure 2-11 – Three sets of βs derived from three measurements over a 4.2-in mortar baseplate at different position/orientation pairs.

2.1.3 Application of the Technology

Application of this technology is straightforward. A list of target positions is developed from some source. In the case of this demonstration, the anomaly list was derived from available magnetometer data and was provided by the ESTCP Program Office. A target file, containing the target location and an optional flag for additional 'stacking' or averaging, for each anomaly is transferred to the system control program which uses the information from the three GPS antennae to guide the operator to position the array over each target in turn. When positioned over the target, two actions are taken. First, a few seconds of platform position and orientation data are collected to later be used to translate the inverted target position, which is, of course, relative to the array, to absolute position and orientation. Then the system steps through the array sensors sequentially, just as in the characterization measurements discussed in the preceding section, and collects decay data from all twenty-five receive coils for each excitation. These data are then stored electronically on the data acquisition computer. Prior to moving to the next target, the vehicle operator evaluates a display of the 25 monostatic signal amplitudes at the first time gate (42 μs) and compares the values to a 'low SNR' threshold (nominally 5 mV/Amp). If a large-amplitude anomaly is clearly not well centered under the array, the vehicle operator can reposition the array and take an additional measurement. This allows the field team to avoid revisiting a target position as a redo. If no amplitude was above the threshold, the vehicle operator may elect to collect additional data for the target prior to leaving the target location.

In the final version of this technology, the facility for conducting the inversion while the operator is driving the array to the next target could be envisioned. For this demonstration, we plan to perform the inversions off-line so that we have the ability to intervene in the automatic process

as required. The EMI and position data will be transferred to the analyst several times each day for near real-time analysis at the demonstration site.

2.1.4 Development of the Technology

The Chemistry Division of NRL has participated in several programs funded by SERDP and ESTCP whose goal has been to enhance the discrimination ability of MTADS for both magnetometer and EMI array configurations. The process was based on making use of both the location information inherent in an item's magnetometry response and the shape and size information inherent in the response to the time-domain electromagnetic induction (EMI) sensors that are part of the baseline MTADS in either a cooperative or joint inversion. In these past efforts, our classification ability has been limited by the information available from the time-domain EMI sensor. Further information regarding the MTADS magnetometer and EM61-MK2 sensor arrays can be found in Reference 2 and the references within.

To make further progress on UXO classification, a sensor with more available information was required. The Geophex, Ltd. GEM-3 sensor is a frequency-domain EMI sensor with up to ten transmit frequencies available for simultaneous measurement of the in-phase and quadrature response of the target. In principle, there is much more information available from a GEM-3 sensor for use in discrimination decisions. However, the commercial GEM-3 sensor is a hand-held instrument with relatively slow data rates and is thus not very amenable to rapid, wide area surveys. ESTCP Project MM-0033, Enhanced UXO Discrimination Using Frequency-Domain Electromagnetic Induction, was funded to overcome this limitation by integrating an array of GEM-3 sensors with the MTADS platform [3]. Further details can be found in References 2 and 3.

Reference 4 compares the detection-only performance of the magnetometer, the second-generation MTADS EM61-MK2, and the GEMTADS arrays to other demonstrators at both of the Standardized UXO Technology Demonstration Sites. All three sensor arrays were also demonstrated in the Spring of 2007 as part of the ESTCP UXO Discrimination Study at the former Camp Sibert [2]. The magnetometer and EM61-MK2 sensor arrays were demonstrated in the Spring of 2009 as part of the ESTCP UXO Classification Study at the former Camp San Luis Obispo [5].

Under SERDP project MM-1315 (EMI Sensor Optimized for UXO Discrimination) and ESTCP project MM-0601, NRL, SAIC, and G&G Sciences have developed a time-domain EMI sensor optimized for the classification of UXO. The TEMTADS array was constructed in 2007 and field tested at the APG Standardized UXO Test Site in June 2008 [6]. After processing, ranked dig lists were generated and submitted to ATC for scoring. The results of the demonstration, as scored by ATC are available in Reference 6. The TEMTADS array was also demonstrated as part of the 2009 ESTCP UXO Classification Study at the former Camp San Luis Obispo, CA [7] and as part of the 2010 ESTCP UXO Classification Study at the former Camp Butner, NC [8]. The results of the APG and SLO demonstrations are discussed in the ESTCP MR-0601 Project Final Report [9].

2.2 ADVANTAGES AND LIMITATIONS OF THE TECHNOLOGY

The TEMTADS Array is designed to combine the data advantages of a gridded survey with the coverage efficiencies of a vehicular system. We expect to collect data equal, if not better, in quality to the best gridded surveys (the relative position and orientation of the sensors will be better than gridded data) while prosecuting many more targets each field day.

There are obvious limitations to the use of this technology. The array is 2-m square in area and mounted on a trailer. Fields where vegetation, topography, or cultural features interfere with the passage of a trailer of that size will not be amenable to the use of the present array. The other serious limitation is anomaly density. For all sensors, there is a limiting anomaly density above which the response of individual targets cannot be separated individually. We have chosen relatively small sensors for this array which should help with this problem but we cannot eliminate it. Recent developments, including solvers designed for classification in multiple-object scenarios such as SAIC-ASAD's multi-target solver, [10] are being evaluated and their performance characteristics in cluttered environments determined.

3.0 PERFORMANCE OBJECTIVES

Performance objectives for this demonstration are given in Table 3-1 to provide a basis for evaluating the performance and costs of the demonstrated technology. These objectives are for the technologies being demonstrated only. Overall project objectives are given in the ESTCP Live Site Demonstrations Plan. Since the TEMTADS is a classification technology, the performance objectives focus on the second step of the UXO survey problem; we assume that the anomalies from all targets of interest have been detected and have been included on the target list we worked from.

3.1 OBJECTIVE: SITE COVERAGE

A list of previously identified anomalies was provided by the Program Office. The expectation was to gather cued data with the TEMTADS system over each of those anomalies.

3.1.1 Metric

Site coverage is defined as the fraction of the assigned anomalies surveyed by the TEMTADS. Exceptions were made for vegetation / topography / cultural interferences.

3.1.2 Data Requirements

The collected data were compared to the original anomaly list. Any interferences were noted in the field log books.

Table 3-1 – Performance Objectives for this Demonstration

Performance Objective	Metric	Data Required	Success Criteria
Quantitative Performance Objectives			
Site Coverage	Fraction of assigned anomalies interrogated	Survey results	100% as allowed for by vegetation /topography / cultural interference
Instrument Verification (IVS) Strip Results	System responses consistent for emplaced items	Daily IVS data	• ≤ 15% RMS variation in β amplitudes • Down-track location ± 25cm
Location Accuracy	Average error and standard deviation in both axes for interrogated items	• Estimated location from analyses • Ground truth from validation effort	ΔN and ΔE < 5 cm σN and σE < 10 cm
Depth Accuracy	Average Error and standard deviation in depth for interrogated items	• Estimated location from analyses • Ground truth from validation effort	ΔDepth < 5 cm σDepth < 10 cm
Production Rate	Number of anomalies investigated each day	• Survey results • Log of field work	125 anomalies/day
Data Throughput	Throughput of data QC process	Log of analysis work	All data QC'ed on site and at pace with survey
Qualitative Performance Objective			
Reliability and Robustness	General Observations	Team feedback and recording of emergent problems	Field team has no significant issues to report

3.1.3 Success Criteria

The objective is considered met if 100% of the assigned anomalies were surveyed with the exception of areas that could not be surveyed due to vegetation / cultural / topography interferences.

3.2 OBJECTIVE: INSTRUMENT VERIFICATION STRIP RESULTS

This objective supports that the sensor system is in good working order and collecting physically valid data each day. The Instrument Verification Strip (IVS) was surveyed twice daily. The amplitude of the derived response coefficients for each emplaced item was compared to the running average for the demonstration for reproducibility. The extracted fit location of each item was compared to the reported ground truth.

3.2.1 Metric

The reproducibility of the measured response of the sensor system to the emplaced items and of the extracted locations of the emplaced items defines this metric.

3.2.2 Data Requirements

The tabulated fit parameters for the data corresponding to each emplaced item in terms of derived response coefficients, location, and depth.

3.2.3 Success Criteria

The objective is considered met if the RMS amplitude variation of the derived response coefficients was less than 15% and the down-track fit locations of the IVS items were within 25 cm of the stated locations.

3.3 OBJECTIVE: LOCATION ACCURACY

An important measure of how efficiently any intrusive investigation will proceed is the accuracy of the predicted locations marked to be dug. Large location errors lead to confusion among the UXO technicians assigned to the effort; costing time and often leading to removal of a small, shallow object when a larger, deeper object was the intended target.

3.3.1 Metric

The average error and standard deviation in both horizontal axes are computed for the items selected for excavation during the validation phase of the demonstration.

3.3.2 Data Requirements

The anomaly fit parameters and the ground truth for the excavated items.

3.3.3 Success Criteria

This objective is considered met if the average error in position for both the Easting and Northing quantities was less than 5 cm and the standard deviation for both was less than 10 cm.

3.4 OBJECTIVE: DEPTH ACCURACY

An important measure of how efficiently any required intrusive investigations will proceed is the accuracy of the predicted depth of the targets marked to be dug. Large depth errors lead to confusion among the UXO technicians assigned to the effort costing time and often leading to removal of a small, shallow object when a larger, deeper object was the intended target.

3.4.1 Metric

The average error and standard deviation of the predicted depths with respect to the ground truth define this metric.

3.4.2 Data Requirements

The anomaly fit parameters and the ground truth for the excavated items.

3.4.3 Success Criteria

This objective is considered met if the average error in depth was less than 5 cm and the standard deviation was less than 10 cm.

3.5 OBJECTIVE: PRODUCTION RATE

This objective considers a major cost driver for the collection of high-density, high-quality geophysical data, the production rate. The faster quality data can be collected without sacrificing field crew safety, the higher the financial return on the data collection effort.

3.5.1 Metric

The number of anomalies investigated per day determined the production rate for a cued survey system.

3.5.2 Data Requirements

The field logs provided the amount of time per day spent acquiring the data and the survey results determined the number of anomalies investigated in that time period.

3.5.3 Success Criteria

This objective is considered met if average production rate was at least 125 anomalies / day.

3.6 OBJECTIVE: DATA THROUGHPUT

The collection of a complete, high-quality data set with the sensor platform is critical to the downstream success of the ESTCP Live Site Demonstrations. This objective considers one of the key data quality issues, the ability of the data analysis workflow to support the data collection

effort in a timely fashion. To maximize the efficient collection of high quality data, a series of standard data quality checks are conducted during and immediately after data collection on site. Data which pass this data quality control (QC) screen are then processed into archival data stores. Analyses are then conducted on those archival data. The data QC / preprocessing portion of the workflow needs to keep pace with the data collection effort for best performance.

3.6.1 Metric

The throughput of the data quality control workflow was at least as fast the data collection process, providing real time feedback to the data collection team of any issues.

3.6.2 Data Requirements

The data analysts log books provide the necessary data.

3.6.3 Success Criteria

This objective is considered met if all collected data were processed through the data quality control portion of the workflow in a timely fashion.

3.7 OBJECTIVE: RELIABILITY AND ROBUSTNESS

This objective represents an opportunity for all parties involved in the data collection process to provide feedback on areas where the process could be improved.

3.7.1 Data Requirements

Discussions with, and/or observations by, the entire field team and other observations were used.

4.0 SITE DESCRIPTION

Please refer to the ESTCP Live Site Demonstrations Plan [1].

5.0 TEST DESIGN

5.1 CONCEPTUAL EXPERIMENTAL DESIGN

The demonstration was executed in two stages. The first stage was to characterize the TEMTADS sensor array with respect to the site-specific items of interest and to the site specific geology. The background response of the demonstration site, as measured by the TEMTADS, was characterized throughout the data collection through the frequent measurement of anomaly-free areas for background subtraction. Characterization of items of interest was done using the preexisting Geophysical Prove Out (GPO, See Section 5.4.4), the Instrument Verification Strip (IVS, see Section 5.4.3), and our existing library of munitions responses.

The second stage of the demonstration was the survey of the demonstration site using the TEMTADS. The array was positioned roughly over the center of each anomaly on the source anomaly list and a data set collected. Each data set was examined to insure that both the GPS and EMI data were of sufficient quality to archive and that the anomaly corresponding to the flag location was fully illuminated. Target parameter estimation, as discussed in the data analysis methodology Section (Section 6.0), was not done as part of this demonstration and is being handled by the data analysis demonstrators directly. The archive data will be submitted to the Program Office when assembled.

The schedule of field testing activities is provided in Figure 5-1 as a Gantt chart.

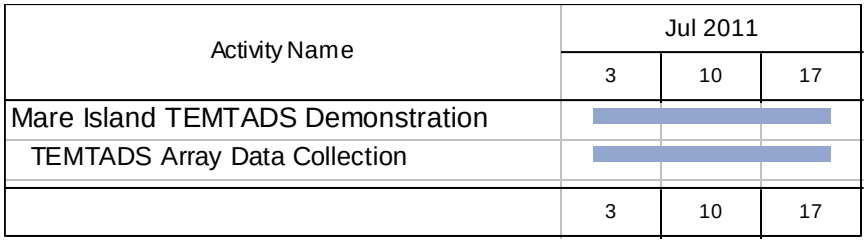

Figure 5-1 – Field Testing Activities Schedule for Mare Island, CA

5.2 SITE PREPARATION

Please refer to the ESTCP Live Site Demonstrations Plan [1].

5.3 SYSTEMS SPECIFICATION

This demonstration was conducted using the NRL MTADS tow vehicle and subsystems. The tow vehicle and each subsystem are described further in the following sections.

5.3.1 MTADS Tow Vehicle

The MTADS has been developed with support from ESTCP. The MTADS hardware consists of a low-magnetic-signature vehicle that is used to tow the different sensor arrays over large areas (10 - 25 acres / day) to detect buried UXO. The MTADS tow vehicle and magnetometer array are shown in Figure 5-2.

5.3.2 RTK GPS System

Positioning is provided using cm-level Real Time Kinematic (RTK) Global Positioning System (GPS) receivers. To achieve cm-level precision, a fixed reference base station is placed on an established first-order survey control point near the survey area. The base station transmits corrections to the GPS rover at 1 Hz via a radio link (450 MHz). The TEMTADS array is located in three-dimensional space using a three-receiver RTK GPS system shown schematically in Figure 2-5 [11]. The three-receiver configuration extends the concept of RTK operations from that of a fixed base station and a moving rover to moving base stations and moving rovers. The

lead GPS antenna (and receiver, Main) receives corrections from the fixed base station. This corrected position is reported at 10-20 Hz using a vendor-specific NMEA-0183 message format (PTNL,GGK or GGK). The Main receiver also operates as a 'moving base,' transmitting corrections (by serial cable) to the next GPS receiver (AVR1) which uses the corrections to operate in RTK mode.

Figure 5-2 – MTADS tow vehicle and magnetometer array.

A vector (AVR1, heading (yaw), angle (pitch), and range) between the two antennae is reported at 10 Hz using a vendor-specific NMEA-0183 message format (PTNL,AVR or AVR). AVR1 also provides 'moving base' corrections to the third GPS antenna (AVR2) and a second vector (AVR2) is reported at 10 Hz. All GPS measurements are recorded at full RTK precision, ~2-5 cm. The GPS position is averaged for 2 seconds as part of the data acquisition cycle. The averaged position and orientation information are then recorded to the position (.gps, ASCII format) data file. The details of the file format are provided in Appendix C.

5.3.3 Time-Domain Electromagnetic Sensor

The TEMTADS Array is a 5 x 5 square array of individual sensors. Each sensor has dimensions of 40 cm x 40 cm, for an array of 2 m x 2 m overall dimensions. The bottom of the array is positioned at a ride height of 17 cm above the ground, unchanged from the former Camp Butner, NC demonstration of 2010 [8]. The rationale of this array design is discussed in Reference 12. The result is a cross-track and down-track separation of 40 cm. Sensor numbering is indicated in Figure 2-5. The transmitter electronics and the data acquisition computer are mounted in the tow vehicle. Custom software written by NRL provides both navigation to the individual anomalies and data acquisition functionality. After the array is positioned roughly centered over the center of the anomaly, the data acquisition cycle is initiated. Each transmitter is fired in a sequence winding outward clockwise from the center position (12). The received signal is recorded for all 25 Rx coils for each transmit cycle. The transmit pulse waveform duration is 2.7 sec (0.9 sec block time, 9 repeats within a block, 3 blocks stacked, with a 50% duty cycle). While it is possible to record the entire decay transient at 500 MHz, we have found that binning the data into 122 time gates simplifies the analysis and provides additional signal averaging without

significant loss of temporal resolution in the transient decays as discussed in Section 2.1.1 [13]. The data are recorded in a binary format as a single file with 25 data points (one data point per Tx cycle). The filename corresponds to the anomaly ID from the target list under investigation.

5.4 CALIBRATION ACTIVITIES

5.4.1 TEMTADS Sensor Calibration

For the TEMTADS, a significant amount of data has been collected with the system as configured at our Blossom Point facility, both on a test stand and in the towed configuration on our test field [14] and during our recent demonstrations at APG [6], SLO [7], and Camp Butner [8]. These data and the corresponding fit parameters provide us with a set of reference parameters including those of clear background (i.e. no anomaly present) and for range scrap and other clutter.

Daily calibration efforts consisted of collecting background (no anomaly) data sets periodically throughout the day at quiet spots to monitor the system noise floor and performance. These quiet spots were deemed to be anomaly-free and, as a result, allowed us to gauge both the levels and spatial/temporal variations of the system noise at the site. The items emplaced in the IVS were measured twice daily to monitor the reproducibility in the system response and to insure proper operation of the array. Variations were expected to be within 15% of the reference values. These two types of measurements constituted the daily calibration activities.

5.4.2 Background Data

A group of anomaly-free areas throughout the demonstration site were identified and characterized using the TEMTADS as required throughout the demonstration. Since they all provided roughly comparable responses, a convenient subset were chosen to be visited periodically throughout the day, on every day of the demonstration. All 124 background measurements taken for the duration of the demonstration (July 5-20, 2011) are shown in Figure 5-3, and are presented as the mean and standard deviation of the 25 monostatic measured signals. Table 5-1 tabulates the intraday variations of the mean and standard deviation quantities from Figure 5-3.

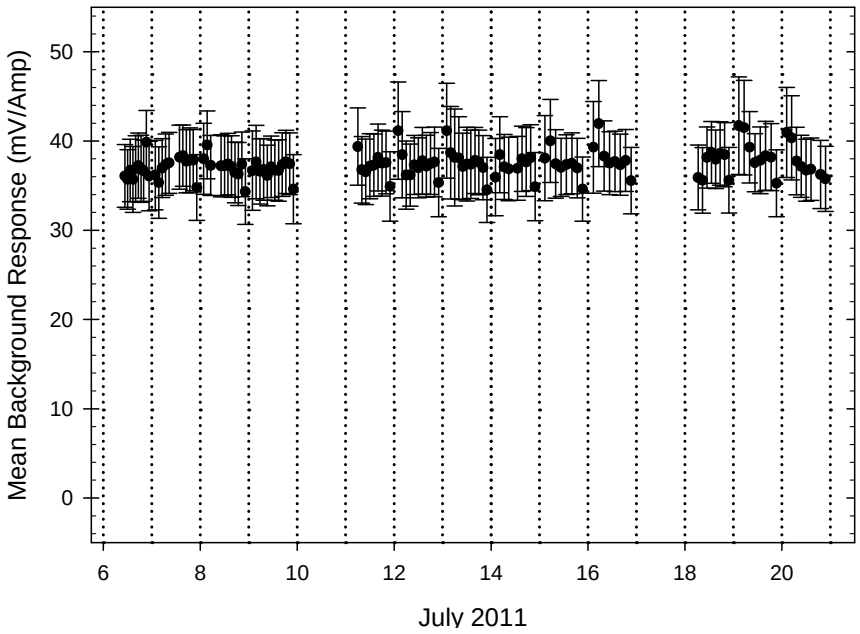

Figure 5-3 – Intra- and inter- daily variations in the response of the TEMTADS to background anomaly-free areas through the duration of the demonstration at fMINSY. The points represent the average measured signal of the 25 monostatic quantities, while the bars represent the standard deviation of those quantities (i.e. 1σ about the mean).

Table 5-1 – Summary of the Daily Variation in the Mean and Standard Deviation of the Signals Measured for the Background Areas.

Date	# of Bkgs.	Mean (mV/Amp)	Std. Dev. (mV/Amp)
7/6/2011	10	36.78	3.60
7/7/2011	11	37.11	3.58
7/8/2011	11	37.12	3.55
7/9/2011	12	36.79	3.65
7/11/2011	10	37.26	3.75
7/12/2011	11	37.43	3.88
7/13/2011	11	37.73	4.25
7/14/2011	9	37.11	3.82
7/15/2011	8	37.38	3.77
7/16/2011	8	38.19	3.93
7/18/2011	8	37.38	3.54
7/19/2011	8	38.72	4.14
7/20/2011	8	37.73	3.93

5.4.3 Instrument Verification Strip Data

The IVS was established to provide a reference against which to verify the repeatability of the system response on several items of interest. Details of the contents of the IVS are given in Table 5-2. Each emplaced item in the IVS was measured twice daily, once before starting the data collection process and a second time before shutting the system down at the end of each day.

The 37mm projectile (37mmP) was obtained from the Aberdeen Test Center stock. The small Industry Standard Object (ISO) is a 1-in nominal, 4-in long pipe nipple[1] that has been described previously [15]. The SuperISO is similar to the small ISO, but 8" long[2].

Table 5-2 – Details of Former Mare Island Naval Shipyard IVS

Target	Description	Easting (m)	Northing (m)	Depth to Bottom of Item (cm)	Orientation	Azimuth	Yaw (deg grid)
1	SuperISO	565,244.43	4,215,473.37	10	Horizontal	Cross	~50
2	37mmP	565,252.62	4,215,464.74	13	Horizontal	Along	~320
3	Small ISO	565,255.82	4,215,461.00	10	Horizontal	Along	~320

All data sets for each of the emplaced IVS items were inverted using the data analysis methodology discussed in Section 6.0, and the estimated target parameters determined. The results are summarized in the following Figures and Tables.

The derived response coefficients (β_1,β_2,β_3) for all 25 data sets taken over the SuperISO over the duration of the demonstration are plotted in Table 5-3. There was a GPS outage during the July 18 PM calibration strip run and these values are not included in these analysis. As expected, the amplitudes of the three coefficients partition into one large and two smaller and approximately equal ones, suggesting a cylindrical shape. The RMS (1σ) variation in the amplitude at 0.042 ms in the decay was that the variation is less than 3% of the mean amplitude for the primary polarizability and ~10% for the secondary polarizabilities (Figure 5-5 and the first entry in Table 5-3). Apart from β_2 and β_3 for the superISO, all RMS variations fall below 7% of the respective mean amplitudes. For all three IVS items, the results convincingly point to a cylindrical shape where β_2 and β_3 are comparable and smaller than β_1.

[1] McMaster-Carr P/N 44615K466, (http://www.mcmaster.com), Pipe size 1", I.D. 1.049", O.D. 1.315", wall thickness 0.133".

[2] McMaster-Carr P/N 4550K233, Pipe size 1", I.D. 0.957", O.D. 1.315", wall thickness 0.179"

Table 5-3 – Summary of the Amplitude Variations at 0.042 ms in the Derived Response Coefficients for All Items Emplaced in the IVS.

Item	β_1 Amplitude (m^3)				β_2 Amplitude (m^3)				β_3 Amplitude (m^3)			
	Min	Max	Mean	RMS	Min	Max	Mean	RMS	Min	Max	Mean	RMS
SuperISO	1.30	1.41	1.33	0.04	0.39	0.53	0.48	0.04	0.33	0.54	0.46	0.06
37mmP	0.57	0.71	0.62	0.02	0.43	0.55	0.47	0.03	0.41	0.49	0.43	0.02
Small ISO	0.50	0.56	0.52	0.01	0.22	0.26	0.23	0.01	0.21	0.24	0.22	0.01

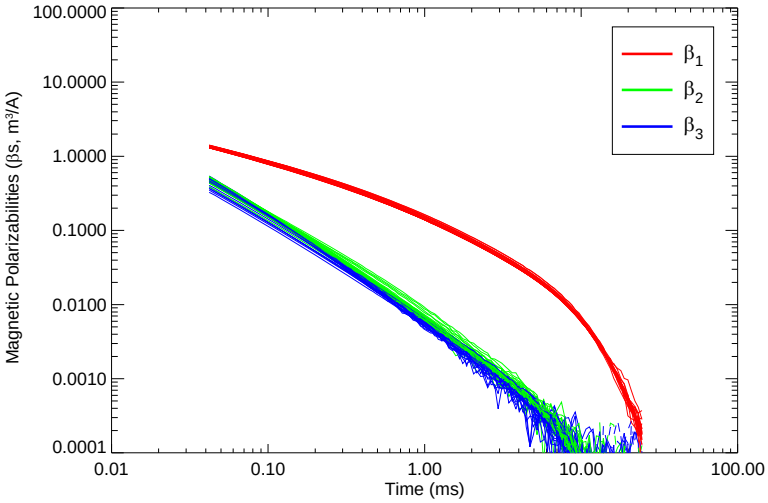

Figure 5-4 – Derived response coefficients for item 1, the superISO, emplaced in the IVS.

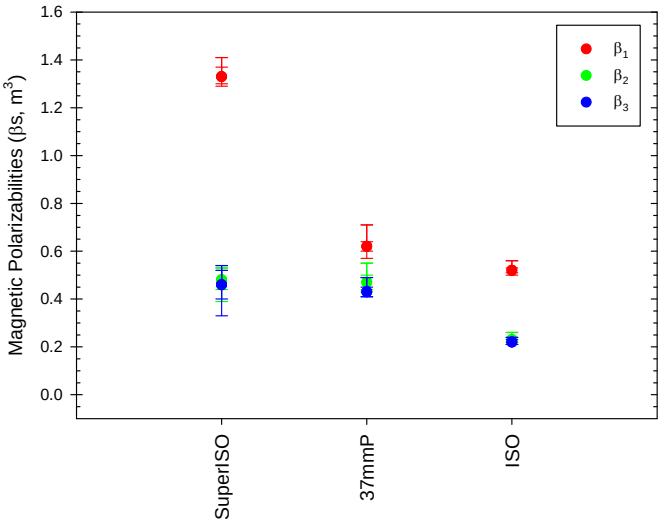

Figure 5-5 – Amplitude variations at 0.042 ms in the derived response coefficients for all items emplaced in the IVS (right panel). β_1 is in red; β_2 is in green; and β_3 is in blue.

The Easting and Northing position errors for all 25 data sets taken over the SuperISO of the IVS over the duration of the demonstration are plotted in the left panel of Figure 5-6. The position error is defined as the fit position (or, equivalently, the inverted position parameter) minus the position given in Table 5-2. The horizontal position error statistics for all three IVS items are listed in Table 5-4 and shown in the left panel of Figure 5-7. Since the position errors are referenced to the mean fitted location, necessarily the mean position error is zero in each case. The RMS variation in the position errors for each emplaced IVS item were all under 2 cm. The depth errors for all 25 SuperISO measurements are shown in the right panel of Figure 5-6.

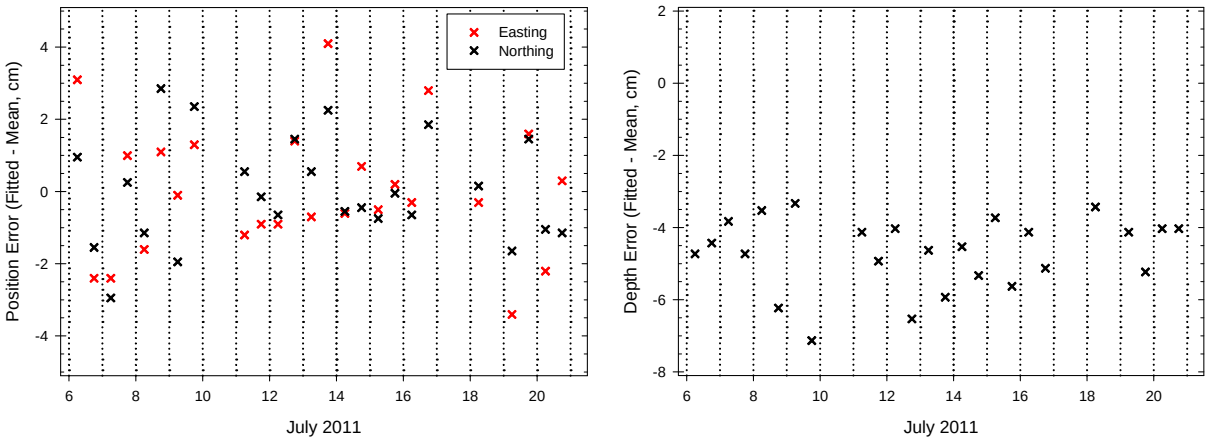

Figure 5-6 – Position errors for the SuperISO emplaced in the IVS (left panel). Easting data are in black and Northing data are in red. Depth errors for the same item (right panel). The depth error statistics for all three IVS items are listed in Table 5-4 and shown in the right panel of Figure 5-7.

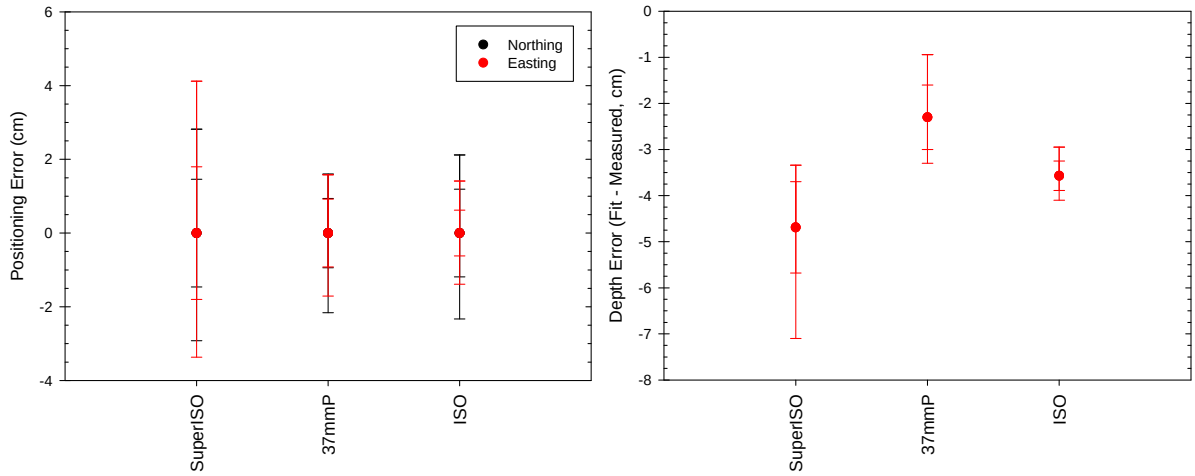

Figure 5-7 – Position error statistics for the three items emplaced in the IVS (left panel). Easting data are in black and Northing data are in red. Depth error statistics for the same items (right panel).

The RMS variation in the depth errors for each emplaced IVS item were all under 1 cm. As Figure 5-6 (right) reveals, there appears to be a roughly -4 cm bias for the depth error for all of the emplaced items. This indicates an offset in either the assumed sensor platform height or some calibration issue in the inversion routines. A mistake in the measured burial depths, while typically a possibility, is unlikely in this case as the IVS was emplaced by this team and the burial depth carefully measured. This will be investigated further.

Table 5-4 – Summary of Position and Depth Error Statistics for all items emplaced in the IVS.

Item	Easting Position Error (cm)				Northing Position Error (cm)				Depth Error (cm)			
	Min	Max	Mean	RMS	Min	Max	Mean	RMS	Min	Max	Mean	RMS
SuperISO	-3.37	4.12	0.00	1.80	-2.92	2.82	0.00	1.46	-7.10	-3.34	-4.69	0.99
37mmP	-1.71	1.58	0.00	0.92	-2.16	1.60	0.00	0.94	-3.30	-0.94	-2.30	0.70
Small ISO	-1.39	1.41	0.00	0.62	-2.33	2.12	0.00	1.19	-4.10	-2.95	-3.57	0.32

5.4.4 Geophysical Prove-Out

There is a previously-emplaced Geophysical Prove-Out (GPO) on site which was used to further populate our reference library of TOI fit parameters. The survey of the GPO was completed at the end of the data collection period. These data will be available as additional training data to the classification demonstrators. Please refer to the ESTCP Live Site Demonstrations Plan for further details. The details of the GPO emplaced at fMINSY are given in Table 5-5, which is adapted from the information provided by site management. The original coordinates were provided in the UTM Zone 10N, NAD83, US survey foot projection. The coordinates presented have been converted into UTM Zone 10N, NAD83, meters and shifted. A long-standing control monument on Mare Island, originally established in 1852, MARE ISLAND SE RESET,[3] was reacquired using the newly established control monument, ESTCP1, as a reference. An offset of 54 cm to the northwest was determined. After failing to find several GPO items at the unshifted coordinates, the offset was applied. The application of the offset led to significantly better positioning of the array with respect to the emplaced items. The details of the shift are given in Table 5-6.

[3] See the National Geodetic Survey Station Datasheet archive at: http://www.ngs.noaa.gov/cgi-bin/ds_desig.prl, NGS Station PID JT00316.

Table 5-5 – fMINSY GPO Details

Seed Item	Easting Shifted (m)	Northing Shifted (m)	Target Description	Proposed Depth (cm)	Orientation (deg)	Azimuth
GPO 1-01	565481.115	4214188.121	3-inch projectile	76	60	E-W
GPO 1-02	565464.235	4214197.111	5-inch projectile	61	45	E-W
GPO 1-03	565451.315	4214188.001	4-inch projectile	91	60	N-S
GPO 1-04	565468.655	4214186.551	40-mm Bofors projectile	36	90	-
GPO 1-05	565477.555	4214185.771	5-inch projectile	122	45	N-S
GPO 1-06	565457.805	4214183.861	8-inch projectile	91	45	N-S
GPO 1-07	565469.295	4214203.451	Projectile fuze	30	90	-
GPO 1-08	565473.315	4214197.701	20-mm Oerlikon case	15	0	N-S
GPO 1-09	565461.125	4214202.131	20-mm Oerlikon round	36	0	E-W
GPO 1-10	565486.205	4214189.701	4-inch projectile	61	90	-
GPO 1-11	565479.465	4214203.651	8-inch projectile	122	30	E-W
GPO 1-12	565481.535	4214209.831	40-mm Bofors case	46	90	-
GPO 1-13	565455.285	4214197.011	8-inch projectile	122	90	-
GPO 1-14	565455.635	4214203.791	40-mm Bofors round	61	60	E-W
GPO 1-15	565463.855	4214202.351	20-mm Oerlikon projectile	30	90	-
GPO 1-16	565464.045	4214194.291	4-inch projectile	30	60	N-S
GPO 1-17	565458.725	4214196.121	6-inch projectile	61	30	N-S
GPO 1-18	565472.685	4214200.511	40-mm Bofors projectile	15	45	N-S
GPO 1-19	565456.595	4214191.991	6-inch projectile	91	90	-
GPO 1-20	565470.045	4214191.901	3-inch projectile	30	45	E-W
GPO 1-21	565469.215	4214205.411	Projectile fuze	15	90	-
GPO 1-22	565484.945	4214201.961	3-inch case	61	90	-
GPO 1-23	565478.265	4214192.691	20-mm Oerlikon round	25	45	N-S
GPO 1-24	565451.725	4214198.391	5-inch projectile	91	90	-
GPO 1-25	565478.505	4214190.691	20-mm Oerlikon projectile	5	45	N-S
GPO 1-26	565481.905	4214196.381	20-mm Oerlikon round	8	0	N-S
GPO 1-27	565482.435	4214195.781	20-mm Oerlikon round	15	0	N-S
GPO 1-28	565482.205	4214197.061	20-mm Oerlikon round	23	0	N-S
GPO 1-29	565482.945	4214196.341	20-mm Oerlikon round	30	0	N-S
GPO 1-30	565482.325	4214194.721	20-mm Oerlikon round	15	0	N-S
GPO 1-31	565448.905	4214199.271	GPO_QC1 (rebar)	0	90	-
GPO 1-32	565474.885	4214191.871	20-mm Oerlikon round	5	0	E-W
GPO 1-33	565471.375	4214198.991	20-mm Oerlikon round	10	0	NE-SW
GPO 1-34	565457.125	4214199.271	20-mm Oerlikon round	10	90	-
GPO 1-35	565464.185	4214185.271	20-mm Oerlikon round	8	30	E-W
GPO 1-36	565486.725	4214197.961	20-mm Oerlikon round	8	45	E-W
GPO 1-37	565472.275	4214189.391	20-mm Oerlikon round	8	60	E-W
GPO 1-38	565453.825	4214200.941	20-mm Oerlikon round	13	0	N-S
GPO 1-39	565475.145	4214194.941	20-mm Oerlikon round	15	90	-
GPO 1-40	565475.635	4214189.011	20-mm Oerlikon round	20	0	N-S
GPO 1-41	565474.105	4214186.541	40-mm Bofors projectile	20	0	N-S
GPO 1-42	565475.475	4214196.411	GPO_QC2 (rebar)	0	90	-
GPO 1-43	565462.315	4214200.111	GPO_QC3 (rebar)	0	90	-

Non-ferrous, may contain some slight ferrous components

Items GPO 1-11 and 1-26 through 1-30 were buried within the utility anomaly

Table 5-6 – Reacquisition Offset for Control Point SE MARE

	UTM Easting (m)	UTM Northing (m)
Reported Position	565,340.500	4,214,585.200
Reacquired Position	565,340.135	4,214,585.601
Offset (Reacq. – Report)	-0.365	0.401

TEM data were not acquired for GPO item 1-14 as it was located several meters into an earthen berm at the north edge of the GPO. After acquiring TEM data over the remaining locations, each data set was QC'ed and then processed by the multi-target solver resident in Geosoft's UX-Analyze add-on for Oasis montaj (v7.3). This was done as a rapid screen to determine which GPO cells contained a target at approximately the reported position and depth and of the correct gauge. A similar analysis was conducted with the original TEMTADS single-solver in IDL for comparison. Twelve positions were found to be empty, GPO 1-01, 1-03 – 1-05, 1-09, 1-11, 1-15, 1-22 – 1-24, 1-28, 1-29. The multi-solver was particularly useful in analyzing several locations where the seed item was small and emplaced at a shallow depth (*e.g.* 20mm projectile) with several other small surface items nearby. Based on the analysis, it was determined that GPO locations 1-08 and 1-12 did not contain an anomaly that was a good match to the reported ground truth. The remaining GPO locations appeared to contain an anomaly that represented a good match to the reported ground truth. Further analysis is left to the data analysis demonstrators.

The details of the discovered positioning offset were presented to the Program Office and the Geometrics MetalMapper team upon the completion of this analysis.

5.5 DATA COLLECTION PROCEDURES

5.5.1 Scale of Demonstration

A cued discrimination survey was conducted within the 61-acre PMA area at the fMINSY of 2,061 previously-identified anomalies. The anomalies were selected from magnetometer data previously collected by the site management team. The resultant anomaly list was provided to the ESTCP Program Office. A subset was selected for this demonstration. The survey was conducted using the NRL TEMTADS. The reproducibility of the system response was determined on a twice-daily basis using the onsite IVS. All data sets were quality checked, located, and background subtracted. The data archives were provided to the ESTCP Program Office.

5.5.2 Sample Density

The EMI data spacing for the TEMTADS is fixed at 40 cm in both directions by the array design.

5.5.3 Quality Checks

Preventative maintenance inspections were conducted at least once a day by all team members, focusing particularly on the tow vehicle and sensor trailer. Any deficiencies were addressed according to the severity of the deficiency. Parts, tools, and materials for many maintenance scenarios were available in the system spares inventory which was located on site. Status on significant break-downs / failures which resulted in long-term delays in operations or degradation of performance were reported to the ESTCP Program Office in a timely fashion.

The data QC procedures were divided into two stages, in-the-vehicle and post-collection, as follows:

The status of the RTK GPS system can be visually determined by the operator prior to starting the data collection cycle, assuring that the position and orientation information are valid, typical Fix Quality (FQ) 3, during the collection period. A Fix Quality (FQ) value of 3 (RTK Fixed) is the best accuracy (typically 3-5 cm or better). A FQ value of 2 (RTK Float) indicates that the highest level of RTK has not been reached yet and location accuracy can be degraded to as poor as ~1 m. FQs 1 & 4 correspond to the Autonomous and DGPS operational modes, respectively.

The vehicle operator has access to a numerical version of the monostatic contour plot, which displays the TEM signal at a decay time of 0.042 ms generated for the 25 transmit/receive pairs to allow for on-the-fly data QC. An example monostatic contour plot for a high SNR anomaly centered under the array is shown in Figure 5-8. The operator display is not current normalized, so the values are expressed in mV. If the anomaly is clearly not well-centered under the array, the vehicle operator can elect to reposition the array accordingly and acquire a second data set.

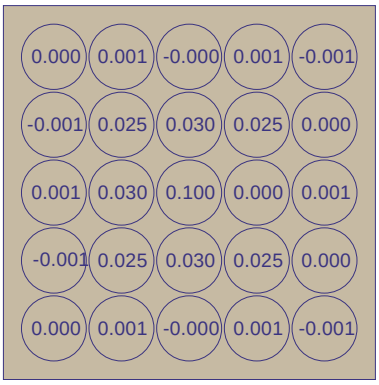

Figure 5-8 – TEMTADS Operator Monostatic Contour Plot
Display with a Single Anomaly Well-Centered under the Array.

Post-collection, three data quality checks were performed on each data set by the Data Analysts. First, the integrity of the GPS positioning information is verified using a software tool written at NRL that checks for common GPS issues (*e.g.*, poor average fix quality). Data collected under FQ 3 and FQ 2 (at the discretion of the data analyst) were retained. For the TEM data, after background subtraction a monostatic contour plot of the TEM signal at a decay time of 0.042 ms was generated for the 25 transmit/receive pairs. The plots were visually inspected to verify that there was a well-defined anomaly without extraneous signals or dropouts. An example is shown in Figure 5-9.

Additionally, a multi-panel plot of the monostatic decay for each sensor was generated. Two examples are shown in Figure 5-10. On the left, the decay plots for the same anomaly as seen in the contour plot in Figure 5-9 are shown. On the right, the decay plots for an anomaly-free, or background, spot are shown. In this case, there was an issue with the decay data from the receiver in sensor #20, leading to a decay that does not match the other 24. For several anomalies

per day, the data were submitted to a dipole inversion routine as an additional QC step. Our experience has been that data glitches also manifest themselves as reduced overall fit coherence (quality).

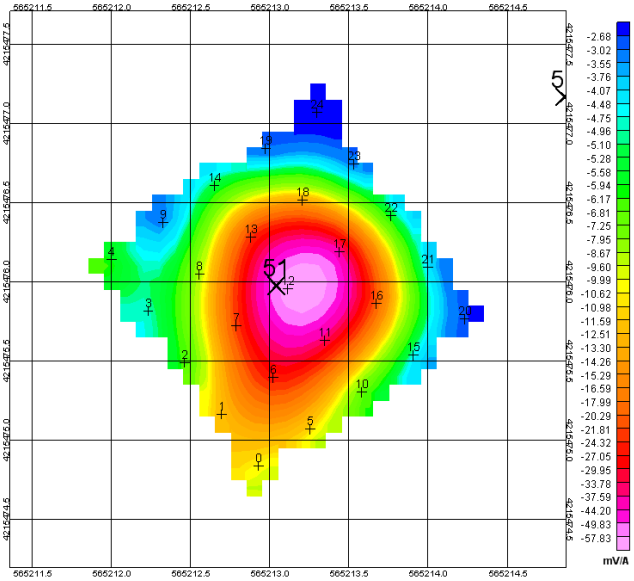

Figure 5-9 – Monostatic contour plot of a well-centered anomaly.

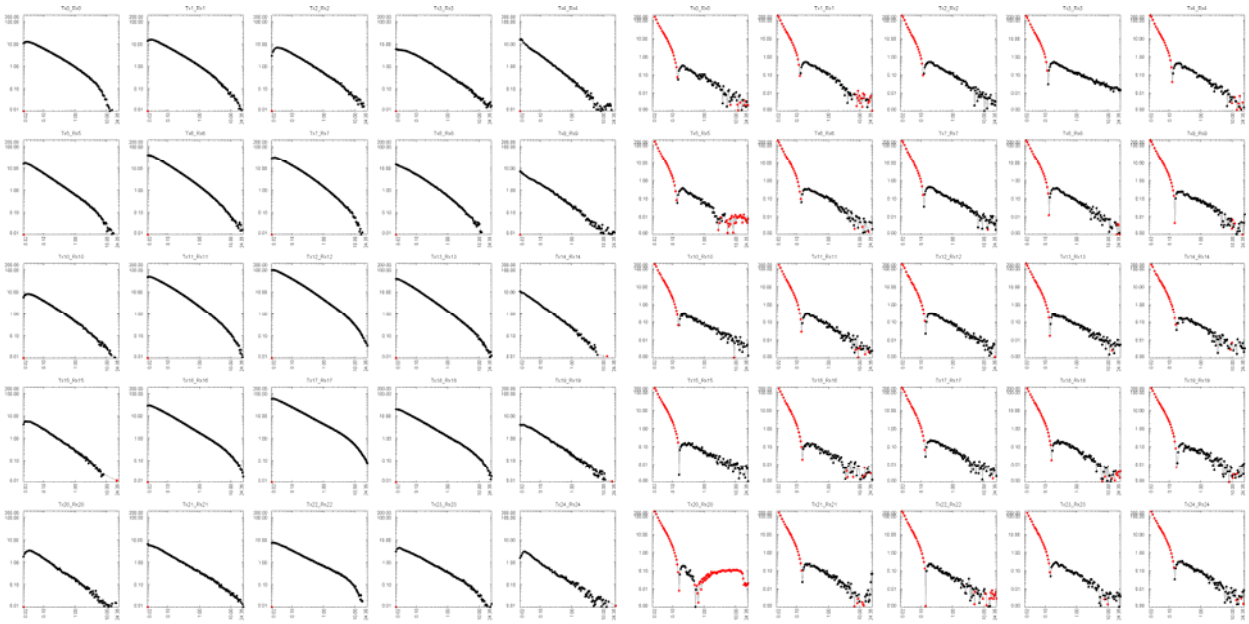

Figure 5-10 – Monostatic decay plots for a) a well-centered anomaly and b) a background (no-anomaly) area with a malfunctioning receiver element (#20).

Any data set which does not pass these QC checks is deemed unsatisfactory by the data analyst and the data are flagged and not processed further. The anomaly ID corresponding to the flagged data is logged for re-acquisition prior to demobilization. Data which do pass these QC checks are of the quality typical of the TEMTADS system, and are sent on to data processing and inversion.

5.5.4 Data Handling

Data were stored electronically as collected on the MTADS vehicle data acquisition computer hard drives. Approximately every two survey hours, the collected data were copied onto removable media and transferred to the data analyst. The data were moved onto the data analyst's computer and the media was recycled. Raw data and analysis results were backed up from the data analyst's computer to external hard disks daily. These results were further archived on an internal file server at SAIC every few days during the demonstration. Examples of the TEMTADS file formats are provided in Appendix C. All field notes / activity logs were written in ink and stored in archival field books. These notebooks are archived at NRL. Relevant sections will be reproduced in demonstration reports, as required. Dr. Tom Bell is the POC for obtaining data and other information. His contact information is provided in Appendix B of this report.

5.6 ANOMALY POSITIONING IN THE PMA

An issue with the locations provided for the items on the anomaly list was identified during the course of the demonstration. First observed by the vehicle operator, there appeared to be a large number of anomalies that were located to the northwest of the provided coordinates. Further review by the data analysts confirmed that there appeared to be a clustering of anomalies that were located roughly 50 cm northwest of the provided coordinates. After discussions by the Program Office with the team that collected the original magnetometer data (Weston), it was determined that none of the control monuments used for the original survey were still in existence. If any had still existed, they could have been used to verify the correspondence between the original and new control networks. There was one long-standing control point available near the PMA, located on the top of the hill at the southern end of the island. This monument was reacquired using control monument "ESTCP1" as a reference. An offset of 54 cm to the northwest was measured. As discussed in Section 5.4.4, application of this offset to the reported locations of the GPO items resolved the positioning issue observed for the GPO. Given the large size of the TEMTADS array and the fact that the seed items had been emplaced using "ESTCP1," it was decided that the remainder of the anomaly list would not be shifted in advance. The downside to this decision was the likely accumulation of addition target flags requiring a second measurement, or redo, due to array mispositioning. In the end, 473 redos were required, significantly higher than for previous demonstrations.

Upon completion of the demonstration, all data sets were batch inverted using the single-source solver in UX-Analyze. The results are shown graphically in Figure 5-11. The horizontal offset between the fit location and the anomaly list position are shown for all targets as small gray circles. All anomalies which met the criteria for being a 'good fit' are shown as larger red circles

on top of the original, gray circles. A 'good fit' is defined in this case as having a) a fit coherence (quality) of ≥ 0.8, b) a fit depth of less than 1.5m, and c) a fit location that was within 0.8m of the center of the array when the data were collected. Two clusters of points were observed in the results and are color-coded for effect. A tight cluster of items is clearly located around the region corresponding to no positioning error (*i.e.*, 0,0). These are color-coded green and likely the seed items as they were recently emplaced using "ESTCP1" as a reference. A second, broader cluster appears to be centered around the point -0.4 m, 0.4 m, or roughly 50 cm northwest of the expected locations and is color-coded dark red. The blue star reflects the measured offset in the location of the control point "SE MARE" as discussed in Section 5.4.4. These items, labeled "Natural Items" may be reflective of compact, metal targets that were in place when the original magnetometer survey was conducted. The remaining bright red circles would most likely represent randomly-distributed surface clutter by the same logic. Once the validation phase of the demonstration is completed, this issue can be revisited.

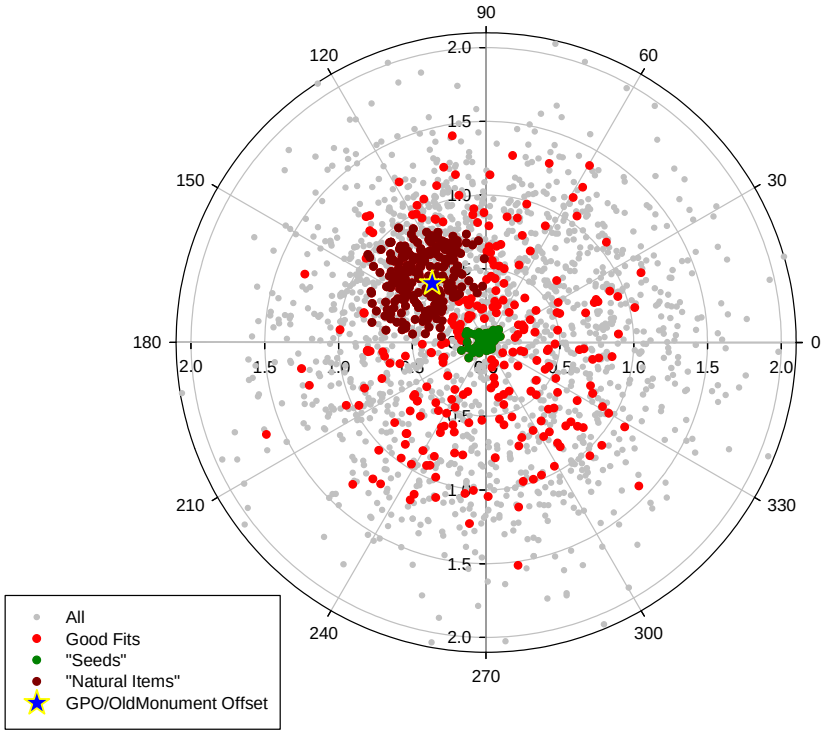

Figure 5-11 – fMINSY TEMTADS Initial Fit Results, Position Error (Horizontal Offset) from the Provided Location.

5.7 VALIDATION

After the completion of all data collection and analysis activities, each anomaly on the master anomaly list that is determined to be reasonable to investigate by the U.S. Navy will be excavated. Each item encountered will be identified, photographed, its depth measured, its location determined using cm-level GPS, and the item removed if possible. All non-hazardous

items will be saved for later in-air measurements as appropriate. This ground truth information, once released, will be used to validate the objectives listed in Section 3.0

6.0 DATA ANALYSIS PLAN

6.1 PREPROCESSING

The TEMTADS array has 25 transmitter/receiver pairs. For each transmit pulse, we record the response at all of the receivers. Hence, for each target we have a 25 x 25 x N data array, where N is the number of recorded time gates. Normally we use 122 logarithmically spaced gates. In preprocessing, the recorded signals are normalized by the transmitter currents to account for any transmitter variations. We subtract 0.028 ms from the nominal gate times to account for time delay due to effects of the receive coil and electronics [16]. The delay was determined empirically by comparing measured responses for test spheres with theory. Measured responses include distortions due to transmitter ringing and related artifacts out to about 0.040 msec. Consequently we only include response beyond 0.040 ms in our analysis. This leaves 115 gates spaced logarithmically between 0.040 ms and 25 ms.

The background response is subtracted from each target measurement using data collected in a nearby target-free region. We evaluated the variability in background measurements and identified outliers which may correspond to measurements over non-ferrous targets by inter-comparing all background measurements. Based on previous experience, we do not observe significant background variability between anomaly-free locations within a given site. This allows us to use measurements from several 100s of meters away for background subtraction on targets.

Geo-referencing of the array data is based on the GPS data, which gives the location of the center of the array and the orientation of the array. Sensor locations within the array are fixed by the array geometry. Dipole inversion of the array data (Section 6.2) determines target location in local array-based coordinates. This will be transformed to absolute coordinates using the array location and orientation determined from the corresponding GPS data.

6.2 PARAMETER ESTIMATION

The raw signature data from the TEMTADS Array reflect details of the sensor/target geometry as well as inherent EMI response characteristics of the targets themselves. In order to separate out the intrinsic target response properties from sensor/target geometry effects we invert the signature data to estimate principal axis magnetic polarizabilities for the targets. The TEMTADS data are inverted using the standard induced dipole response model wherein the effect of eddy currents set up in the target by the primary field is represented by a set of three orthogonal magnetic dipoles at the target location [17]. The measured signal is a linear function of the induced dipole moment **m**, which can be expressed in terms of a time dependent polarizability tensor **B** as

$$\mathbf{m} = \mathbf{U}\mathbf{B}\mathbf{U}^{T}\cdot\mathbf{H}_0$$

where **U** is the transformation matrix between the physical coordinate directions and the principal axes of the target and $\mathbf{H}_0$ is the primary field strength at the target. The eigenvalues $\beta_i(t)$ of the polarizability tensor are the principal axis polarizabilities.

Given a set of measurements of the target response with varying geometries or "look angles" at the target, the data can be inverted to determine the (X,Y,Z) location of the target, the orientation of its principal axes (ϕ,θ,ψ), and the principal axis polarizabilities (β_1,β_2,β_3). The basic idea is to search out the set of nine parameters ($X,Y,Z,\phi,\theta,\psi,\beta_1,\beta_2,\beta_3$) that minimizes the difference between the measured responses and those calculated using the dipole response model.

For the TEMTADS array data, inversion is accomplished by a two-stage method. In the first stage, the target's (X,Y,Z) dipole location is solved for non-linearly. At each iteration within this inversion, the nine element polarizability tensor (**B**) is solved linearly. We require that this tensor be symmetric; therefore, only six elements are unique. Initial guesses for X and Y are determined by a signal-weighted mean. The routine normally loops over a number of initial guesses in Z, keeping the result giving the best fit as measured by the chi-squared value. The non-linear inversion is done simultaneously over all time gates, such that the dipole (X,Y,Z) location applies to all decay times. At each time gate, the eigenvalues and angles are extracted from the polarizability tensor.

In the second stage, six parameters are used: the three spatial parameters (X,Y,Z) and three angles representing the yaw, pitch, and roll of the target (Euler angles ϕ,θ,ψ). Here the eigenvalues of the polarizability tensor are solved for linearly within the 6-parameter non-linear inversion. In this second stage both the target location and its orientation are required to remain constant over all time gates. The value of the best fit X,Y,Z from the first stage, and the median value of the first-stage angles, are used as an initial guess for this stage. Additional loops over depth and angles are included to better ensure finding the global minimum.

Figure 6-1 shows an example of the principal axis polarizabilities determined from TEMTADS array data. The target, a mortar fragment, is a slightly bent plate about 0.5 cm thick, 25 cm long, and 15 cm wide. The red curve is the polarizability when the primary field is normal to the surface of the plate, while the green and blue curves correspond to cases where the primary field is aligned along each of the edges.

Not every target on the target list will have a strong enough TEM response to support extraction of target polarizabilities. All of the data will be run through the inversion routines, and the results will be manually screened to identify those targets that cannot be reliably parameterized. Several criteria will be used in this process: signal strength relative to background, dipole fit error (difference between data and model fit to data), and the visual appearance of the polarizability curves.

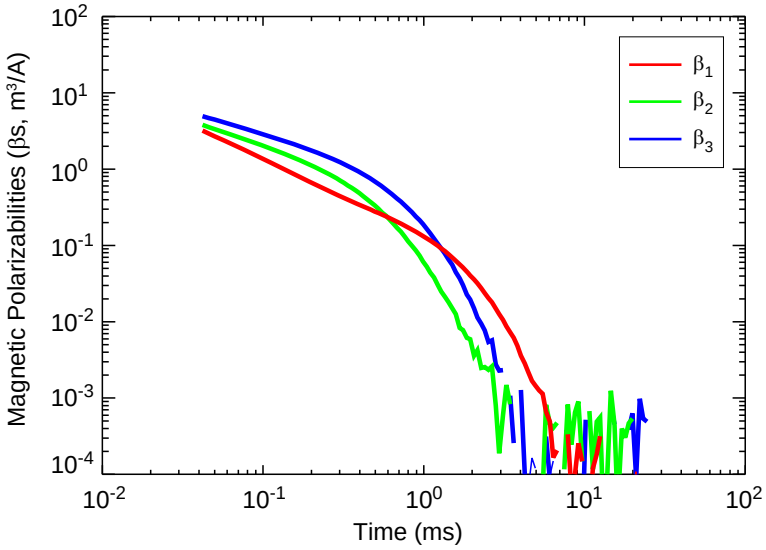

Figure 6-1 – Principal axis polarizabilities for a 0.5 cm thick by 25 cm long by 15 cm wide mortar fragment.

6.3 DATA PRODUCT SPECIFICATIONS

See Appendix C for the detailed data product specifications.

7.0 PERFORMANCE ASSESSMENT

The performance objectives for this demonstration were summarized in Table 3-1, and are repeated here as Table 7-1. The results for each criterion are then discussed in the following sections.

7.1 OBJECTIVE: SITE COVERAGE

A list of previously identified anomalies was provided by the Program Office. The expectation was to gather cued data with the TEMTADS over each of those anomalies.

7.1.1 Metric

Site coverage is defined as the fraction of the assigned anomalies surveyed by the TEMTADS. Exceptions were made for vegetation / topographical /cultural interferences.

7.1.2 Data Requirements

The collected data were compared to the original anomaly list. All interferences were noted in the field log books.

Table 7-1 – Performance Results for this Demonstration.

Performance Objective	Metric	Data Required	Success Criteria	Success?
Quantitative Performance Objectives				
Site Coverage	Fraction of assigned anomalies interrogated	Survey results	100% as allowed for by vegetation / topography / cultural interference	Yes
Instrument Verification Strip (IVS) Results	System responses consistent for emplaced items	Daily IVS data	• ≤ 15% RMS variation in β amplitudes • Down-track location ± 25cm	• Yes • Yes
Location Accuracy	Average error and standard deviation in both axes for interrogated items	• Estimated location from analyses • Ground truth from validation effort	ΔN and ΔE < 5 cm σN and σE < 10 cm	N/A
Depth Accuracy	Average error and standard deviation in depth for interrogated items	• Estimated location from analyses • Ground truth from validation effort	ΔDepth < 5 cm σDepth < 10 cm	N/A
Production Rate	Number of anomalies investigated each day	• Survey results • Log of field work	125 anomalies/day	Yes
Data Throughput	Throughput of data QC process	Log of analysis work	All data QC'ed on site and at pace with survey	Yes
Qualitative Performance Objective				
Reliability and Robustness	General Observations	Team feedback and recording of emergent problems	Field team has no significant issues to report	Yes

7.1.3 Success Criteria

The objective was considered met if 100% of the assigned anomalies were surveyed with the exception of areas that could not be surveyed due to vegetation / topography / cultural interferences.

7.1.4 Results

This objective was successfully met. Of the list provided by the Program Office, all anomalies were investigated. 269 anomalies were not accessible to the array due primarily to cultural

interferences such as buildings or pilings. In some cases there was insufficient GPS coverage to insure that the array was in the correct position.

7.2 OBJECTIVE: INSTRUMENT VERIFICATION STRIP RESULTS

This objective supports that the sensor system is in good working order and collecting physically valid data each day. The IVS was surveyed twice daily. The amplitude of the derived response coefficients for each emplaced item was compared to running averages for the demonstration for reproducibility. The extracted fit location of each item was compared to the reported ground truth.

7.2.1 Metric

The reproducibility of the measured response of the sensor system to the emplaced items and of the extracted locations of the emplaced items defines this metric.

7.2.2 Data Requirements

The tabulated fit parameters for the data corresponding to each emplaced item in terms of derived response coefficients, location, and depth.

7.2.3 Success Criteria

The objective is considered met if the RMS amplitude variation of the derived response coefficients was less than 15% and if the down-track fit locations of the IVS items were within 25 cm of the stated locations.

7.2.4 Results

As discussed in Section 5.4.3, all RMS amplitude variations fell below the 15% cutoff. The RMS amplitude variation for the β_2 and β_3 coefficients for the SuperISO were 8 and 13%, respectively (refer to Table 5-3). The amplitude variation for the other cases were 6.5% or lower. Referring to Table 5-4, it is clear that the down-track fit locations of each item were well within 2 cm of the stated location, and so the second criterion was also met.

7.3 OBJECTIVE: LOCATION ACCURACY

An important measure of how efficiently any intrusive investigation will proceed is the accuracy of the predicted locations marked to be dug. Large location errors lead to confusion among the UXO technicians assigned to the effort; costing time and often leading to removal of a small, shallow object when a larger, deeper object was the intended target.

7.3.1 Metric

The average error and standard deviation in both horizontal axes are computed for the items selected for excavation during the validation phase of the demonstration.

7.3.2 Data Requirements

The anomaly fit parameters and the ground truth for the excavated items.

7.3.3 Success Criteria

This objective is considered met if the average error in position for both the Easting and Northing quantities was less than 5 cm and the standard deviation for both was less than 10 cm.

7.3.4 Results

The data for determining the success of this objective are not currently available. When the data are available, the analysis can be revisited.

7.4 OBJECTIVE: DEPTH ACCURACY

An important measure of how efficiently any required intrusive investigation will proceed is the accuracy of the predicted depth of the targets marked to be dug. Large depth errors lead to confusion among the UXO technicians assigned to the effort costing time and often leading to removal of a small, shallow object when a larger, deeper object was the intended target.

7.4.1 Metric

The average error and standard deviation of the predicted depths with respect to the ground truth define this metric.

7.4.2 Data Requirements

The anomaly fit parameters and the ground truth for the excavated items.

7.4.3 Success Criteria

This objective is considered met if the average error in depth was less than 5 cm and the standard deviation was less than 10 cm.

7.4.4 Results

The data for determining the success of this objective are not currently available. When the data are available, the analysis can be revisited.

7.5 OBJECTIVE: PRODUCTION RATE

This objective considers a major cost driver for the collection of high-density, high-quality geophysical data, the production rate. The faster data can be collected without sacrificing crew safety or data quality, the higher the financial return on the data collection effort.

7.5.1 Metric

The number of anomalies investigated per day determines the production rate for a cued survey system.

7.5.2 Data Requirements

The field logs provided the amount of time per day spent acquiring the data and the survey results determined the number of anomalies investigated in that time period.

7.5.3 Success Criteria

This objective is considered met if the average production rate was at least 125 anomalies / day.

7.5.4 Results

This objective was successfully met. A total of 2,519 anomalies (including redos) were measured over a 13-day run for an average of 194 anomalies/day.

7.6 OBJECTIVE: DATA THROUGHPUT

The collection of a complete, high-quality data set with the sensor platform is critical to the downstream success of the ESTCP Live Site Demonstrations. This objective considers one of the key data quality issues, the ability of the data analysis workflow to support the data collection effort in a timely fashion. To maximize the efficient collection of high quality data, a series of standard data quality check are conducted during and immediately after data collection on site. Data which pass this data QC screen are then processed into archival data stores. Analyses are then conducted on those archival data. The data QC / preprocessing portion of the workflow needs to keep pace with the data collection effort for best performance.

7.6.1 Metric

The throughput of the data quality control workflow was at least as fast as the data collection process, providing real time feedback to the data collection team of any issues.

7.6.2 Data Requirements

The data analysts log books provide the necessary data.

7.6.3 Success Criteria

This objective is considered met if all collected data were processed through the data quality control portion of the workflow in a timely fashion.

7.6.4 Success Criteria

This objective was successfully met. Data were normally downloaded several times during each workday, and quality control on these datasets was usually completed by the following morning. Quality control checks successfully caught missed anomalies, a small number of corrupt data files, and targets which required additional information or a repositioning of the array. Due to the increased workload caused by trying to resolve the positioning offset discussed in Section 5.6 and the associated increase in potential redos, a third part-time data analyst who was available on site assisted for the second half of the demonstration to maintain the pace.

7.7 OBJECTIVE: RELIABILITY AND ROBUSTNESS

This objective represents an opportunity for all parties involved in the data collection process to provide feedback on areas where the process could be improved.

7.7.1 Data Requirements

Discussions with, and/or observations by, the entire field team and other observations were used.

7.7.2 Results

This objective was successful. As this demonstration was a cooperative effort with NAEVA Geophysics in technology transfer, a significant fraction of the data collection and the majority of the data preprocessing / QC was conducted by NAEVA Geophysics staff with training and assistance from NRL and SAIC. Initial training was conducted on February 10, 2011 at our home facility at Blossom Point. The remainder of the training was conducted hands-on during the demonstration. At the completion of the demonstration, the NAEVA Geophysics staff was asked for any feedback / suggestions to improve the system / process. The team was generally pleased with the system and had no major recommendations for the improvement of the system itself.

The TEMTADS tow vehicle and sensor array controls are complicated systems to operate and navigate. Over the course of the first week, the NAEVA data collection operator was able to become sufficiently comfortable with operating the system to reach a sustainable production level in most situations. Some of the areas at fMINSY were so cluttered / obstructed with cultural items / debris that our more experienced driver was called on exclusively to operate the vehicle in those areas. In any future demonstrations, additional time and training for vehicle operators should be factored into the field schedule.

The demonstration also marked the first field trial of the data QC tools recently developed for the UX-Analyze add-on for Geosoft's Oasis montaj (v7.3). The original QC software, which runs in ITT-VIS's IDL, was available on site to the SAIC data analyst for side-by-side comparisons. A list of issues and feature requests was developed and forwarded to the UX-Analyze development team based on this field trial. Due to the complex nature of the fMINSY site, several typically routine analyses were more involved. For example, the question of how to quantify what an

acceptable background mean and variation were was more difficult in the highly cluttered environment of fMINSY.

The remainder of suggestions focused on better preparation of the site for this kind of demonstration. While these suggestions are outside the scope of this report and effort, several are of note and are cataloged here. First, presumably the team that collected the original magnetometer data collected information about cultural interferences such as surface blocks of concrete, areas of pavement, etc. Capturing that information and providing it to the demonstration teams prior to deployment would have been beneficial. In particular, some target locations in the southern portion of the site were located on the pier or on steel-reinforced concrete. Advanced access to the cultural data could have allowed these locations to be identified in advance and potentially for a decision as to the value of investigating those locations. Lastly, in NAEVA's experience, cueing an EMI survey from magnetometer data is sufficiently difficult that they would recommend reacquiring the anomalies with an EM61-MK2 prior to the cued survey at a minimum.

8.0 COST ASSESSMENT

The cost elements that were tracked during this demonstration are detailed in Table 7-1. The provided cost elements are based on a three-person field crew (2 data collection and 1 data analyst). The costs of two half-time advisors to train the crew on the TEMTADS are included as part of this demonstration.

Table 8-1 – Tracked Costs

Cost Element	Data Tracked	Cost
Data Collection Costs		
Pre/Post Survey Activities	Component costs and integration costs • Spares and consumables	 $10,500
	Cost to pack the array and equipment, mobilize to the site, and return • Personnel required to pack • Packing hours • Personnel to mobilize • Mobilization hours • Transportation costs	$34,750 1 40 5 8 $23,750
	Cost to assemble the system, perform initial calibration tests • Personnel required • Hours required	$1,100 4 2
Survey Costs	Unit cost per anomaly investigated. This will be calculated as daily survey costs divided by the number of anomalies investigated per day. • Preventative maintenance costs (day) • Daily calibration (hours) • Survey personnel required • Survey hours per day • Daily equipment break-down and storage (hours)	**$21.50 / anom.** $600 1 2.5 8 0.5
Processing Costs		**$17.20 / anom.**
Preprocessing	Time required to perform standard data clean up and to merge the location and geophysical data.	3 min/anomaly
Parameter Estimation	Time required to extract parameters for all anomalies.	2 min/anomaly

9.0 SCHEDULE OF ACTIVITIES

Figure 8-1 gives the overall schedule for the demonstration including deliverables.

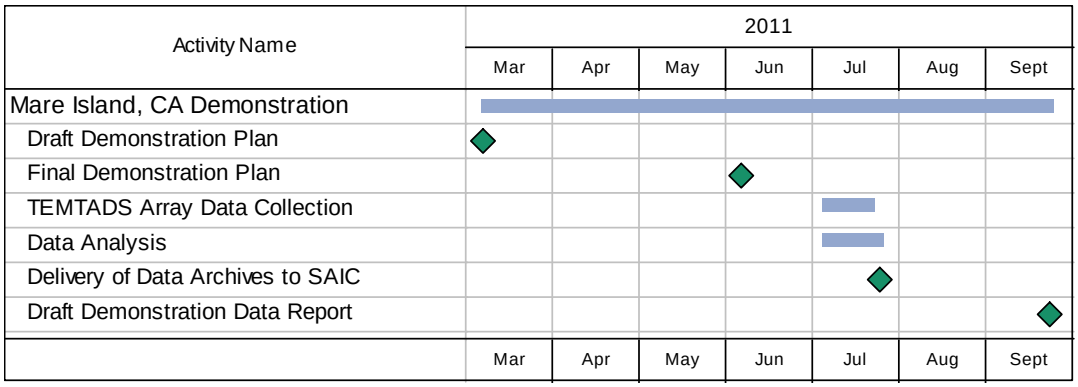

Figure 9-1 – Schedule of all demonstration activities including deliverables.

10.0 MANAGEMENT AND STAFFING

The responsibilities for this demonstration are outlined in Figure 10-1. Dan Steinhurst is the PI of this demonstration. Dan Steinhurst filled the roles of Site / Project Supervisor and assisted with data analysis in the second half of the demonstration. Tom Bell was the Quality Assurance Officer. Glenn Harbaugh served as the Site Safety Officer and as one of the Data Acquisition Operators. His duties included data collection and safety oversight for the entire team. Mark Howard was the second Data Acquisition Operator. Jim Kingdon and Cora Blits served as the Data Analysts.

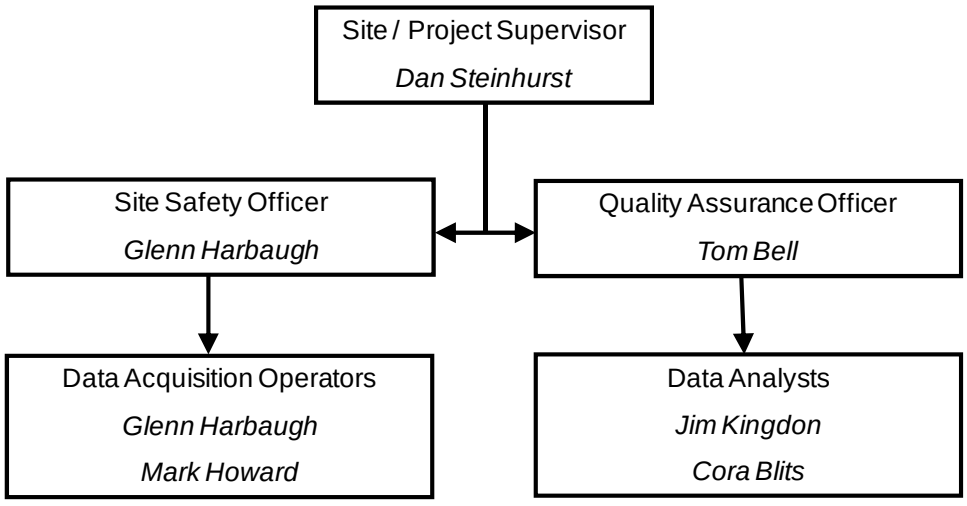

Figure 10-1 – Management and Staffing Wiring Diagram.

11.0 REFERENCES

1. "ESTCP Munitions Response, Live Site Demonstrations, Demonstration Plan, former Mare Island Naval Shipyard, CA," Draft 2, May 5, 2011.

2. "MTADS Demonstration at Camp Sibert Magnetometer / EM61 MkII / GEM-3 Arrays," Demonstration Data Report, G.R. Harbaugh, D.A. Steinhurst, N. Khadr, August 21, 2008.

3. "Enhanced UXO Discrimination Using Frequency-Domain Electromagnetic Induction," ESTCP MM-0033 Final Report, June 27, 2007.

4. "Survey of Munitions Response Technologies," ESTCP, ITRC, and SERDP, June, 2006.

5. "ESTCP MM-0744, Demonstration Data Report, Former Camp San Luis Obispo, Magnetometer and EM61 MkII Surveys," G.R. Harbaugh, N. Khadr, and D.A. Steinhurst, accepted May 7, 2010.

6. "STANDARDIZED UXO TECHNOLOGY DEMONSTRATION SITE SCORING RECORD NO. 920 (NRL)," J.S. McClung, ATC-9843, Aberdeen Test Center, MD, November, 2008.

7. "ESTCP MM-0744, Demonstration Data Report, Former Camp San Luis Obispo, TEMTADS Cued Survey," G.R. Harbaugh, D.A. Steinhurst, D.C. George, J.B. Kingdon, D.A. Keiswetter, and T.H. Bell, accepted May 7, 2010.

8. "2010 ESTCP UXO Classification Study, Rougemont, NC, ESTCP MR-1034, Data Demonstration Report, Former Camp Butner, MTADS Discrimination Array (TEMTADS) Survey," N. Khadr, J.B. Kingdon, G.R. Harbaugh, and D.A. Steinhurst, NRL Memorandum Report NRL/MR/6110—11-9366, Naval Research Laboratory, Washington, DC, October 20, 2011.

9. "EMI Array for Cued UXO Discrimination, ESTCP MM-0601, Final Report," D.C. George, J.B. Kingdon, T. Furuya, D.A. Keiswetter, T.H. Bell, G.R. Harbaugh, and D.A. Steinhurst, Naval Research Laboratory Memorandum Report NRL/MR/6110--10-9289, September 16, 2010.

10. "Source Separation using Sparse-Solution Linear Solvers," J.T. Miller, D.A. Keiswetter, J.B. Kingdon, T. Furuya, B.J. Barrow, and T.H. Bell, *Detection and Sensing of Mines, Explosive Objects, and Obscured Targets XV*, Proc. of SPIE Vol. *7664*, 766409 (**2010**).

11. "Moving Platform Orientation for an Unexploded Ordnance Discrimination System," D. Steinhurst, N. Khadr, B. Barrow, and H. Nelson, *GPS World*, **2005**, *16/5*, 28 – 34.

12. “Array Specification Report,” H.H. Nelson, ESTCP Project MM-0601, June, 2007.

13. ESTCP In-Progress Review, H.H. Nelson, ESTCP Project MM-0601, March 1, 2007.

14. “Design and Construction of the NRL Baseline Ordnance Classification Test Site at Blossom Point,” H.H. Nelson and R. Robertson, Naval Research Laboratory Memorandum Report NRL/MR/6110—00-8437, March 20, 2000.

15. “EM61-MK2 Response of Three Munitions Surrogates,” H.H. Nelson, T. Bell, J. Kingdon, N. Khadr, D.A. Steinhurst, NRL Memorandum Report NRL/MR/6110--090-9183, Naval Research Laboratory, Washington, DC, March 12, 2009.

16. "Time and Frequency Domain Electromagnetic Induction Signatures of Unexploded Ordnance," T. Bell, B. Barrow, J. Miller, and D. Keiswetter, Subsurface Sensing Technologies and Applications Vol. 2, No. 3, July 2001.

17. "Subsurface Discrimination Using Electromagnetic Induction Sensors," T.H. Bell, B.J. Barrow, and J.T. Miller, *IEEE Transactions on Geoscience and Remote Sensing*, Vol. *39*, No. *6*, June **2001**.

APPENDIX A. HEALTH AND SAFETY PLAN (HASP)

An abbreviated Health and Safety Plan was generated for this demonstration. All emergency information such as contact numbers and directions to nearby medical facilities are provided in that document. The contents are reproduced here.

A.1 DIRECTIONS TO THE HOSPITAL

Directions to the Sutter Medical Center are as follows, starting on Railroad Ave northwest of the work site. See Figure A-1 for the overall route.

1) Head NORTHWEST on Railroad Ave towards 10th Street, go 1.9 miles.
2) Take the ramp onto CA-37 E, go 2.0 miles.
3) Take Exit 19 for CA-29 towards Napa, go 0.3 miles.
4) Merge onto Lewis Brown Drive, go 0.3 miles.
5) Take a sharp right onto Broadway Street, go 0.3 miles.
6) Turn left onto Tuolumne Street, got 0.9 miles.
7) Turn left onto Hospital Drive, go 0.1 miles.
8) Take a slight right turn onto Los Cerritos Drive, go 60 feet.
9) Take a slight left turn onto Hospital Drive, go 200 feet.
10) Arrive at Sutter Medical Center.

Sutter Medical Center is located at 300 Hospital Drive, Vallejo, CA 94589, 707-554-4444. The total distance to travel is 5.9 miles and should take 14 minutes.

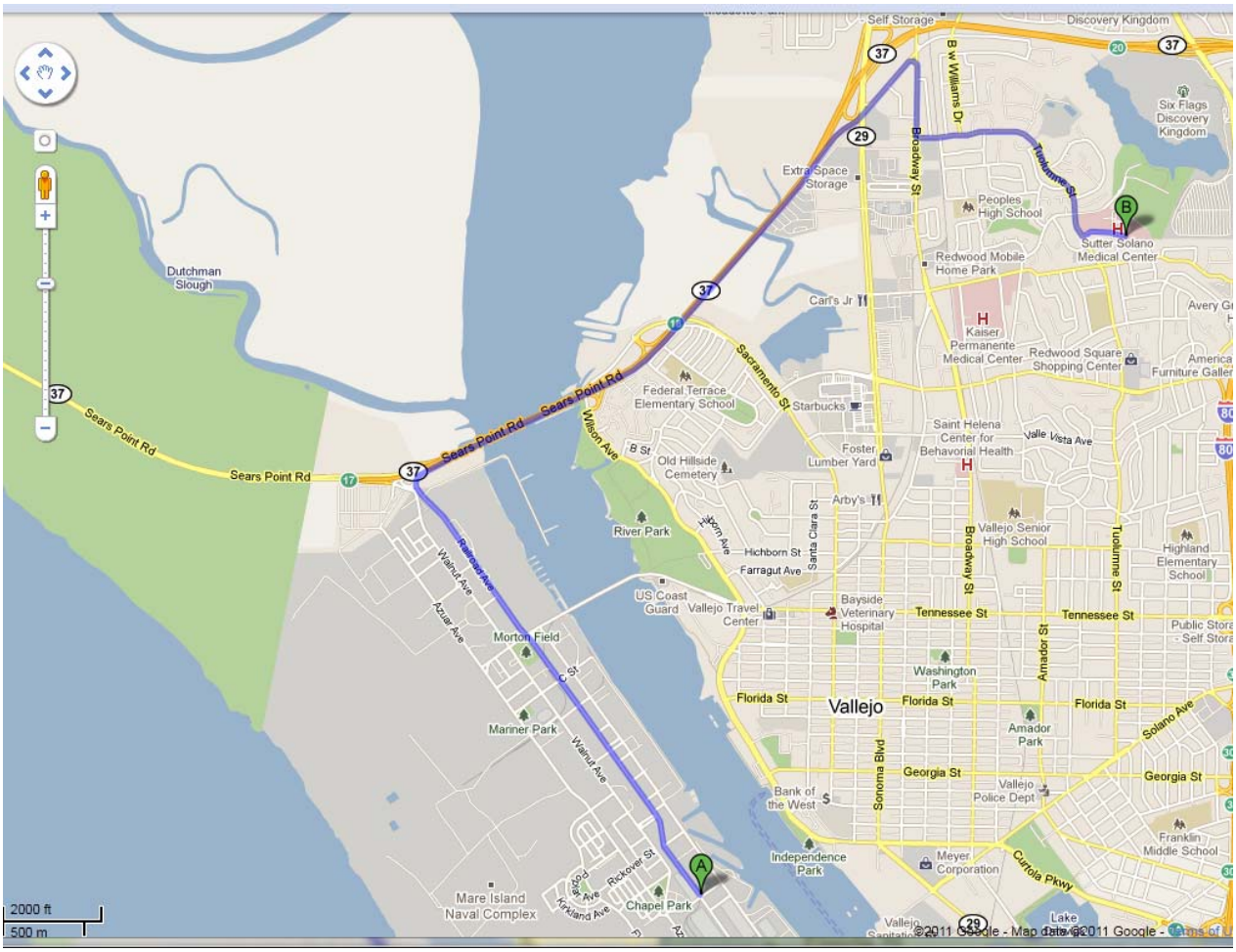

Figure A-1 – Area map showing the location of the Sutter Medical Center with respect to the work site.

A.2 EMERGENCY TELEPHONE NUMBERS

Telephone numbers for medical fire and other emergencies will be available on site for use by all project personnel in the event of an emergency and are provided in Table A-1. All vehicles will contain a cellular phone (including the phone list) to allow emergency communications in the event of an accident. The telephone area code for this area is 707.

Table A-1 – Emergency Contact Numbers

Agency	Emergency Phone Number	Non-Emergency Phone Number	Location
Vallejo Fire Department	911	(707) 648-4526	970 California Avenue, Vallejo, CA 94590
Ambulance	911		
Police Department	911	(707) 648-4321	111 Amador Street, Vallejo, CA 94590
Sutter Medical Center		(707) 554-4444	300 Hospital Drive, Vallejo, CA 94589
Walgreens Pharmacies (24 Hr.)		(707) 557-694	1050 Redwood Street, Vallejo, CA 94590
California Poison Action Line		(800)-222-1222	

APPENDIX B. POINTS OF CONTACT

POINT OF CONTACT	ORGANIZATION	Phone Fax e-mail	Role in Project
Dr. Jeff Marqusee	ESTCP Program Office 901 North Stuart Street, Suite 303 Arlington, VA 22203	703-696-2120 (V) 703-696-2114 (F) jeffrey.marqusee@osd.mil	Director, ESTCP
Dr. Anne Andrews	ESTCP Program Office 901 North Stuart Street, Suite 303 Arlington, VA 22203	703-696-3826 (V) 703-696-2114 (F) anne.andrews@osd.mil	Deputy Director, ESTCP
Dr. Herb Nelson	ESTCP Program Office 901 North Stuart Street, Suite 303 Arlington, VA 22203	703-696-8726 (V) 703-696-2114 (F) 202-215-4844 (C) herbert.nelson@osd.mil	Program Manager, MR
Ms. Katherine Kaye	HydroGeoLogic, Inc. 11107 Sunset Hills Road, Suite 400 Reston, VA 20190	410-884-4447 (V) kkaye@hgl.com	Program Manager Assistant, MR
Mr. Daniel Reudy	HydroGeoLogic, Inc. 11107 Sunset Hills Road, Suite 400 Reston, VA 20190	703-736-4531 (V) druedy@hgl.com	Program Manager's Assistant, MR
Dr. Dan Steinhurst	Nova Research, Inc. 1900 Elkin St., Ste. 230 Alexandria, VA 22308	202-767-3556 (V) 202-404-8119 (F) 703-850-5217 (C) dan.steinhurst@nrl.navy.mil	PI
Mr. Glenn Harbaugh	Nova Research, Inc. 1900 Elkin St., Ste. 230 Alexandria, VA 22308	804-761-5904 (V) glenn.harbaugh.ctr@nrl.navy.mil	Site Safety Officer
Dr. Tom Bell	SAIC - ASAD 4001 N. Fairfax Drive, 4th Floor Arlington, VA 22203	(703)-312-6288 (V) thomas.h.bell@saic.com	Quality Assurance Officer
Mr. John Breznick	NAEVA Geophysics, Inc. P.O. Box 7325 Charlottesville, VA 22906	(434) 978-3187 ext. 206 (V) (434) 825- 8175 (C) (434) 973-9791 (F) jbreznick@naevageophysics.com	General Manager

APPENDIX C. DATA FORMATS

C.1 POSITION / ORIENTATION DATA FILE (*.GPS)

```
Antenna,X_Offset,Y_Offset,Z_Offset,Easting/Yaw,Northing/Pitch,HAE/Range
Main,0.000,1.365,0.730,316256.990,4254211.094,-25.934
AVR1,-0.778,-1.418,0.740,3.40349,0.00761,2.882
AVR2,0.778,-1.418,0.745,1.55718,0.00425,1.554
```

These data files are ASCII format, comma-delimited files. A header line is provided.

Line 1 – Header information

Line 2 – Main GPS antenna data

```
Main              - Antenna Identifier
0.000             - Cross-track distance from array center
1.365             - Down-track distance from array center
0.730             - Vertical distance from array center
316256.990        - Easting (UTM, m) position of Main antenna
4254211.094       - Northing (UTM, m) position of Main antenna
-25.934           - Height-above-ellipsoid (m) position of Main antenna
```

Line 3 & 4 – AVR GPS antenna data (AVR1 as example)

```
AVR1              - Antenna Identifier
-0.778            - Cross-track distance from array center
-1.418            - Down-track distance from array center
0.740             - Vertical distance from array center
3.40349           - Yaw of AVR vector (radians, True North referenced)
0.00761           - Pitch of AVR vector (radians)
2.882             - Range of AVR vector (m)
```

C.2 TEM DATA FILE (*.TEM)

These data files are a binary format generated by a custom .NET serialization routine. They are converted to an ASCII, comma-delimited format in batches as required. Each file contains 25 data points, corresponding to each Tx cycle. Each data point contains the Tx transient and the corresponding 25 Rx transients as a function of time. A pair of header lines is also provided for, one overall file header and one header per data point with the data acquisition parameters. A partial example is provided below.

Line 1 - File Header

```
CPUms,PtNo,LineNo,Delt,BlockT,nRepeats,DtyCyc,nStk,AcqMode,GateWid,Gate
HOff,TxSeq,GateT,TxI_Z,Rx0Z_TxZ,Rx1Z_TxZ,Rx2Z_TxZ,Rx3Z_TxZ,Rx4Z_TxZ,Rx5
Z_TxZ,Rx6Z_TxZ,Rx7Z_TxZ,Rx8Z_TxZ,Rx9Z_TxZ,Rx10Z_TxZ,Rx11Z_TxZ,Rx12Z_TxZ
,Rx13Z_TxZ,Rx14Z_TxZ,Rx15Z_TxZ,Rx16Z_TxZ,Rx17Z_TxZ,Rx18Z_TxZ,Rx19Z_TxZ,
Rx20Z_TxZ,Rx21Z_TxZ,Rx22Z_TxZ,Rx23Z_TxZ,Rx24Z_TxZ,
```

Line 2 - Data Point Header

```
0,1,0,2E-06,0.9,9,0.5,3,2,0.05,5E-05,22,

0           - Start time in ms on CPU clock (always 0)
1           - Data Point Number (always 1)
0           - Line Number (always 0)
2E-06       - Time step for transients (seconds)
0.9         - Base period length (seconds)
9           - Number of Tx cycles in a base period
0.5         - Duty cycle
3           - Number of base periods averaged (or stacked)
2           - Data Acquisition Mode (binned)
0.05        - Gate width as fraction of its own time
5E-05       - Hold-off time (seconds) for first data point
22          - Tx ID number (sensor number + 10)
```

Line 3 - First Data Line in First Data Point

```
,,,,,,,,,,,,2.5E-05,2.01102465120852,-4.71949940100108E-05,-
1.79793904939509E-05,1.39366551389817E-05,-2.55470612811271E-05,-
4.84779418501355E-05,4.05641650778409E-05,6.73185201421361E-06,-
0.000116516308079121,-2.49295973312366E-06,4.21216420108736E-
05,3.70976690069955E-05,-0.000127606649206979,-0.000510366345393333,-
0.000100251591870083,5.19149917311475E-05,3.71239440686929E-05,-
6.05368361143584E-06,-0.000125671808025774,2.44747669528873E-
05,5.7401043406257E-05,-5.14479298585597E-05,-9.42595187481444E-
06,3.27817636140336E-05,-1.1886747308274E-05,-5.57022247620241E-05,
```

C.3 LEVELED DATA FILE

Prior to any analysis of the .TEM data files, the data are background-subtracted and normalized for transmitter power. These leveled data sets are also provided in an Geosoft Oasis montaj .XYZ file format. The self-explanatory header row and one line of data are provided below.

```
/  ----------------------------------------------------------------------
---------
/ CSV EXPORT [08/16/2011]
/ DATABASE   [.\Temtads_data.gdb]
/  ----------------------------------------------------------------------
---------
/
/X,Y,Z,Tx,Rx,Data_lev[0],Data_lev[1],Data_lev[2],Data_lev[3],Data_lev[4
],Data_lev[5],Data_lev[6],Data_lev[7],Data_lev[8],Data_lev[9],Data_lev[
10],Data_lev[11],Data_lev[12],Data_lev[13],Data_lev[14],Data_lev[15],Da
ta_lev[16],Data_lev[17],Data_lev[18],Data_lev[19],Data_lev[20],Data_lev
[21],Data_lev[22],Data_lev[23],Data_lev[24],Data_lev[25],Data_lev[26],D
ata_lev[27],Data_lev[28],Data_lev[29],Data_lev[30],Data_lev[31],Data_le
v[32],Data_lev[33],Data_lev[34],Data_lev[35],Data_lev[36],Data_lev[37],
Data_lev[38],Data_lev[39],Data_lev[40],Data_lev[41],Data_lev[42],Data_l
ev[43],Data_lev[44],Data_lev[45],Data_lev[46],Data_lev[47],Data_lev[48]
,Data_lev[49],Data_lev[50],Data_lev[51],Data_lev[52],Data_lev[53],Data_
lev[54],Data_lev[55],Data_lev[56],Data_lev[57],Data_lev[58],Data_lev[59
],Data_lev[60],Data_lev[61],Data_lev[62],Data_lev[63],Data_lev[64],Data
_lev[65],Data_lev[66],Data_lev[67],Data_lev[68],Data_lev[69],Data_lev[7
0],Data_lev[71],Data_lev[72],Data_lev[73],Data_lev[74],Data_lev[75],Dat
a_lev[76],Data_lev[77],Data_lev[78],Data_lev[79],Data_lev[80],Data_lev[
81],Data_lev[82],Data_lev[83],Data_lev[84],Data_lev[85],Data_lev[86],Da
ta_lev[87],Data_lev[88],Data_lev[89],Data_lev[90],Data_lev[91],Data_lev
[92],Data_lev[93],Data_lev[94],Data_lev[95],Data_lev[96],Data_lev[97],D
ata_lev[98],Data_lev[99],Data_lev[100],Data_lev[101],Data_lev[102],Data
_lev[103],Data_lev[104],Data_lev[105],Data_lev[106],Data_lev[107],Data_
lev[108],Data_lev[109],Data_lev[110],Data_lev[111],Data_lev[112],Data_l
ev[113],Data_lev[114],Data_lev[115],Data_lev[116],Data_lev[117],Data_le
v[118],Data_lev[119],Data_lev[120]
565144.921,4215491.234,0.296,0,0,-1.341,-2.147,-1.960,-1.152,-0.764,-
0.614,-0.425,-0.316,-0.315,-0.317,-0.329,-0.330,-0.349,-0.402,-0.406,-
0.436,-0.415,-0.370,-0.380,-0.372,-0.369,-0.351,-0.336,-0.330,-0.243,-
0.232,-0.184,-0.189,-0.210,-0.169,-0.203,-0.210,-0.210,-0.177,-0.221,-
0.196,-0.227,-0.147,-0.169,-0.128,-0.139,-0.184,-0.131,-0.107,-0.096,-
0.099,-0.126,-0.098,-0.118,-0.093,-0.080,-0.093,-0.100,-0.078,-0.068,-
0.054,-0.078,-0.042,-0.050,-0.025,-0.038,-0.036,-0.045,-0.034,-0.041,-
0.044,-0.021,-0.042,-0.035,-0.016,-0.001,-0.027,-0.026,-0.025,-0.032,-
0.033,-0.032,-0.016,-0.003,0.009,-0.013,-0.004,-0.011,-0.013,-0.005,-
0.026,-0.018,-0.026,-0.019,-0.009,-0.007,-0.004,-0.016,-0.019,-0.005,-
0.005,-0.017,-0.001,-0.007,0.002,0.011,-0.001,0.005,-0.002,-
0.003,0.011,0.010,0.007,0.010,0.005,0.001,0.010,-
0.001,0.006,0.006,0.001,0.006,0.007,0.009,0.009,0.007
```